

RESEARCH

Open Access



New tetrahydroisoquinolines bearing nitrophenyl group targeting HSP90 and RET enzymes: synthesis, characterization and biological evaluation

Etify A. Bakhite^{1*} , Reda Hassanien², Nasser Farhan², Eman M. Sayed^{2*} and Marwa Sharaky³

Abstract

In this study, new tetrahydroisoquinoline compounds were synthesized by reaction of 7-Acetyl-4-cyano-1,6-dimethyl-6-hydroxy-8-(3-nitrophenyl or 4-nitrophenyl)-5,6,7,8-tetrahydroisoquinoline-3(2*H*)-thiones with methyl iodide, chloro acetonitrile, ethyl chloroacetate to produce compounds **3–5** and reacted with *N*-arylchloroacetamides reagents to give tetrahydroisoquinolin-3-ylthio) acetamides compounds **6a–c**, **8a–b** which can cyclized to 6,7,8,9-tetrahydrothieno[2,3-*c*]isoquinoline-2-carboxamides compounds **7a–c**, **9a–b**. Also react with *N*-(benzthiazol-2-yl)-2-chloroacetamide to give compound **10**. The structures of all newly synthesized compounds were characterized by elemental and spectral analyses. Also, most of the synthesized compounds were evaluated for their anticancer activities against **MCF7** and **HEPG2** cell lines. From the result we found that the most active compound against the **MCF7** cell lines was compound **8b**, and the most active compound against **HEPG2** cell lines was compound **3**. Then the effects of compound **3** on the **HEPG2** cell line was investigated using an apoptotic Annexin V-FITC test and flow cytometry. Compound **3** induced a 59-fold increase in **HEPG2** cell line apoptosis and cell cycle arrested at the G0-G1, G2/M phases. Moreover, the molecular docking study was applied and the result showed that compounds **8b** bind to the RET enzyme with binding energies of -6.8 kcal/mol in comparison with standard **alectinib**, which exhibits a binding energy of -7.2 kcal/mol. Compound **3** can bind with **HSP 90** with a binding energy (ΔG) of -6.8 kcal/mol, which was comparable to the standard **Onalespib** (-7.1 kcal/mol).

Keywords Anticancer, Apoptosis, Cell cycle, RET enzyme (rearranged during transfection) enzyme, Heat shock protein (**HSP90**) enzyme, **HEPG2** cell line, **MCF7** cell line, Tetrahydroisoquinoline

*Correspondence:

Etify A. Bakhite
etafy@aun.edu.eg

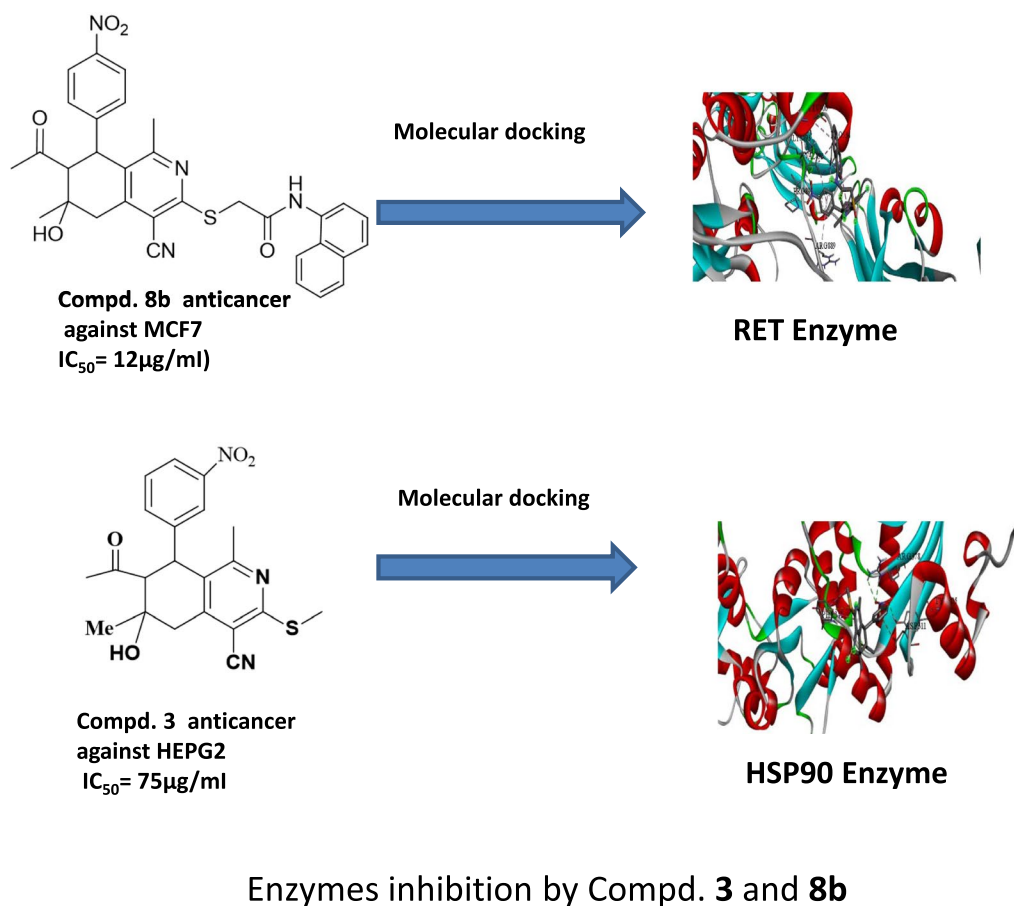
Eman M. Sayed
Emanmohsen@sci.nvu.edu.eg

Full list of author information is available at the end of the article



© The Author(s) 2025. **Open Access** This article is licensed under a Creative Commons Attribution 4.0 International License, which permits use, sharing, adaptation, distribution and reproduction in any medium or format, as long as you give appropriate credit to the original author(s) and the source, provide a link to the Creative Commons licence, and indicate if changes were made. The images or other third party material in this article are included in the article's Creative Commons licence, unless indicated otherwise in a credit line to the material. If material is not included in the article's Creative Commons licence and your intended use is not permitted by statutory regulation or exceeds the permitted use, you will need to obtain permission directly from the copyright holder. To view a copy of this licence, visit <http://creativecommons.org/licenses/by/4.0/>.

Graphical Abstract



Introduction

Cancer is unbalanced cell proliferation results from changes in genetic expression, which causes cells to divide uncontrollably [1, 2]. Cancer is a form of hereditary disease. It is the main factor that causes mortality and morbidity [3]. Treating cancer diseases has been an important issue [4]. Common method, such as surgery, chemotherapy, and radiotherapy were used but in recent years more safe methods for cancer treatment are favorable like stem cell therapy, targeted therapy, ablation therapy, nanoparticles, natural antioxidants and new anticancer chemical compounds [4].

Liver cancer is the most prevalent cause of cancer-related fatalities, and it ranks sixth in the US [5]. Only this cancer has an annual percentage rise in frequency among the top five deadly cancers [6, 7]. Developed countries have Liver diseases are more common in developing nations [8]. Liver cancer can be caused by hepatitis B and C viruses [9], fatty liver disease, cirrhosis

caused by alcohol [7], smoking, obesity, diabetes, iron overload, and other dietary exposures are risk factors. Nevertheless, the success rate of chemotherapeutic therapy is less than one-third of patients, and after a few months of the program's initiation, medication resistance develops [10, 11]. Eating more fruits and vegetables reduces the chance of acquiring cancer, according to a European study [10–12]. Some chemicals exhibited cytotoxicity to cancer cells while leaving non-cancerous cells unharmed [13] such as Piperine, inhibits enzymes required for drug metabolism, implying that co-administration with existing chemotherapeutic medicines may be used to raise plasma concentrations [14]. Furthermore, polysaccharides derived from *Tricholoma matsutake* and *Lentinus edodes* enhance the inhibitory effect of 5-fluorouracil (5-FU) [15]. Moreover, tetrahydroisoquinoline compounds have the potential to treat liver cancer. For example, 3-arylisoquinoline-based natural products based on corydamine

exhibited a significant inhibitory effect, and mechanistic studies suggested that the compound was a dual inhibitor of Topo I and Topo II, with Topo II inhibitory activity [16]. Additionally, the 1-styrenyl isoquinoline compound demonstrated anticancer properties against Huh7 and SK-Hep-1 cells [17].

Breast cancer is the most frequent type of cancer in women worldwide, accounting for 2.26 million cases annually, 11.7% of all cancer cases, and 24.5% of female cancer cases [18, 19]. Cytotoxic chemotherapy medications, including capecitabine, 5-fluorouracil (5-FU), doxorubicin, epirubicin, gemcitabine, methotrexate, paclitaxel, tamoxifen citrate, and nucleosides, are the standard treatment for breast cancer [20]. They are still considered hazardous compounds even though they have been linked to negative long-term side effects [20, 21]. An ongoing research project is underway to develop effective new drugs or improve chemotherapy regimens.

A new compounds derivative based on tetrahydro-[1,2,4]triazolo[3,4-a]isoquinolin-3-yl)-3-arylprop-2-en-1-one was produced and evaluated on mouse (Luc-4T1) and human (MDA-MB-231) breast cancer cell lines [18]. Also, a cycloplatinated (II) complex based on isoquinoline alkaloid induces ferritinophagy-dependent ferroptosis in triple-negative breast cancer cells [22].

Another, methods for decrease cancer diseases spreading are inhibition the enzymes responsible for cancer multiplicity and spreading like DHFR, CDK2, RET, TULBIN, HSP90, HSP70, EGR...etc.

A molecular chaperone known as heat shock protein 90 (HSP90) is required for the stability and functionality of a number of conditionally activated and/or expressed signaling proteins [23, 24], as well as a number of mutant, chimeric, or overexpressed signaling proteins that promote the survival, proliferation, or both of cancer cells [25]. Through their specific engagement with a single molecular target, HSP90 inhibitors inactivate, disrupt, and eventually destroy HSP90 client proteins. It has shown promising antitumor potential in preclinical model systems [26–28].

The tyrosine kinase receptor, or RET, often engages in interactions with ligands at the cell surface and is essential for a variety of cellular processes, including as migration, metabolism, survival, differentiation, and proliferation [29]. At every stage of life, RET is expressed, starting at the very beginning of embryogenesis. A variety of aggressive diseases, such as Hirschsprung disease and cancer, are brought on by mutations that either activate or suppress RET [29]. Because the RET receptor is essential for hunger, weight gain management, and the survival and maintenance of multiple sclerosis, its important to inhibit RET enzyme to decrease disease spreading specially cancer diseases [30].

The 5,6,7,8-tetrahydroisoquinoline ring system is a structural element of numerous alkaloids [31, 32]. 5,6,7,8-Tetrahydroisoquinoline compounds have biological activities like enzyme inhibitors against many types of enzymes like DHFR, CDK2, RET, HSP90, EGFR and tulbin [33–36] and viral infections [37]. Also the were reported to have anticonvulsant properties [38]. Antibacterial [39], neurotropic [40], and antibacterial properties [41]. Also, 5,6,7,8-tetrahydroisoquinoline compounds have been used as anticancer agents [42–44].

On the other hand, numerous nitro-group-containing compounds have been shown to have a wide range of applications in biochemistry and medicine, including antioxidants and anticancers [45–48].

In light of the foregoing discoveries and as a continuation of our previous [49–52] work on tetrahydroisoquinolines, the purpose of this research was to synthesize and analyze the title compounds in the hope that these new compounds will find useful applications as anticancer drugs. And the difference between this work and pervious nitrophenyl tetrahydroisoquinoline work are: (a) In this article we synthesized meta and para tetrahydroisoquinolines but in the previous study we use ortho, tetrahydroisoquinolines. (b) We used different cell lines HEPG2, MCF7. (c) We used different enzymes RET and HSP90.

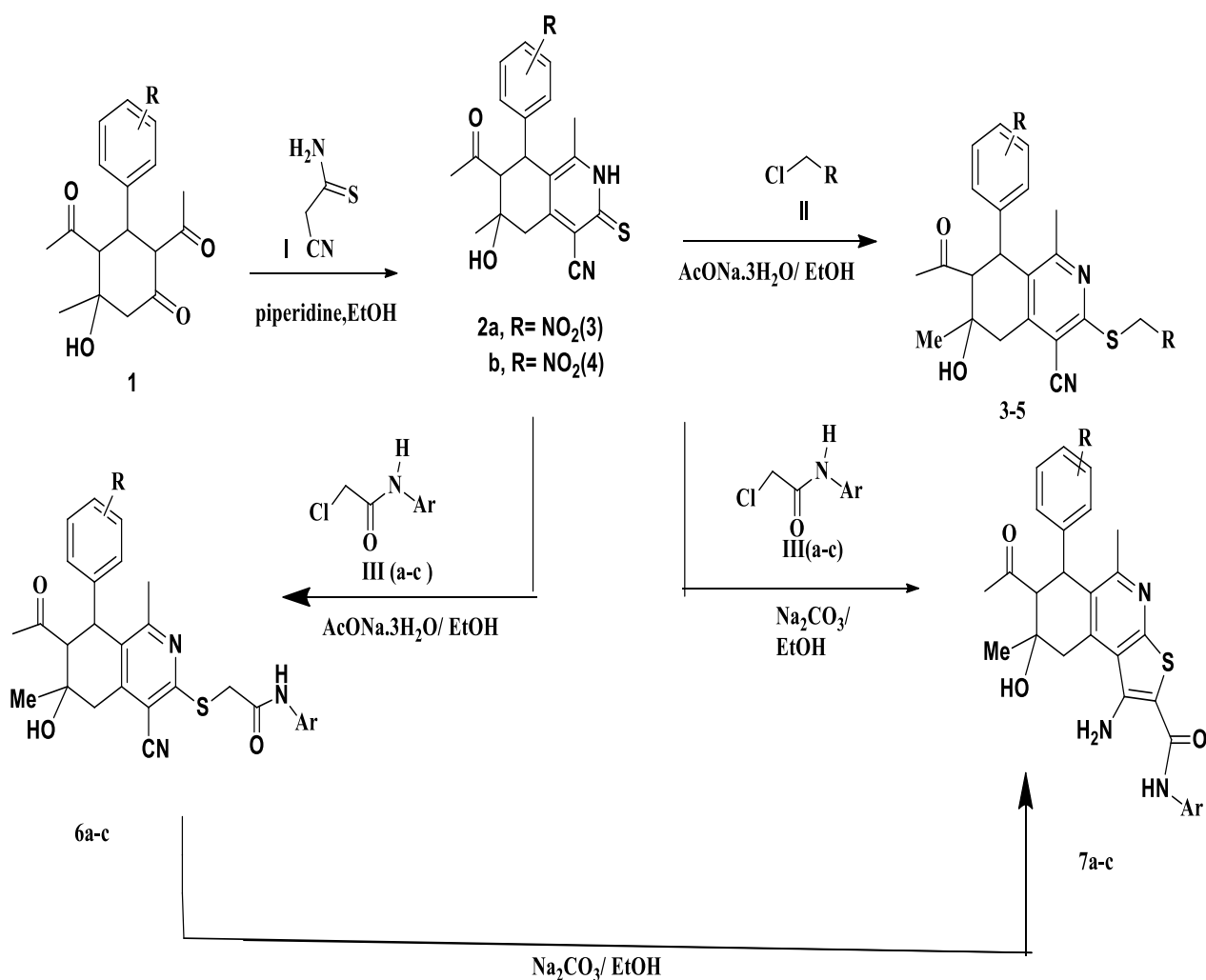
Results and discussion

Synthesis part

Cyclocondensation of 2,4-diacetyl-5-hydroxy-5-methyl-3-(2-nitrophenyl, 3-nitrophenyl, or 4-nitrophenyl) cyclohexanones **1a–b** with 2-cyanothioacetamide by refluxing in ethanol using piperidine as a basic catalyst formed the starting components are 7-acetyl-4-cyano-1,6-dimethyl-6-hydroxy-8-(3-nitrophenyl, or 4-nitrophenyl)-5,6,7,8-tetrahydroisoquinoline-3(2H)-thiones **2a–b** (Scheme 1).

Refluxing compounds **2a–b** with halocompounds like methyl iodide, ethyl chloroacetate, and chloroacetonitrile in ethanol with slightly excess sodium acetate trihydrate for one hour resulted in the formation of 3-(un)substituted methylthio-5,6,7,8-tetrahydroisoquinoline-4-carbonitriles **3–5** (Scheme 1).

Also, compounds **2a–b** reacted with *N*-aryl-2-chloroacetamides **III(a–c)** to produce the corresponding *N*-aryl-(5,6,7,8-tetrahydroisoquinolin-3-ylthio)acetamides **6a–c** in excellent yields. Compounds **6a–c** undergo cyclization by heating with catalytic quantities of sodium ethoxide in sodium carbonate 3 h to provide the equivalent 7-acetyl-1-amino-*N*-aryl-5,8-dimethyl-8-hydroxy-6-(3-nitrophenyl/4-nitrophenyl)-6,7,8,9-tetrahydrothieno[2,3-*c*]isoquinoline-2-carboxamides **7a–c**. Compounds **7a–c** were also synthesized via heating



Compd.	R	Yield %	compd.	R	Ar	compd.	Ar
3	H	NO ₂ (3)	6a,7a	NO ₂ (3)	C ₆ H ₅ COMe	III(a)=III(b)	C ₆ H ₅ COMe
4	CO ₂ Et	NO ₂ (3)	6b,7b	NO ₂ (4)	C ₆ H ₅ COMe	III(c)	C ₆ H ₅ Cl
5	CN	NO ₂ (4)	6c	NO ₂ (4)	C ₆ H ₅ Cl		
			7c	NO ₂ (3)	C ₆ H ₅ Cl		

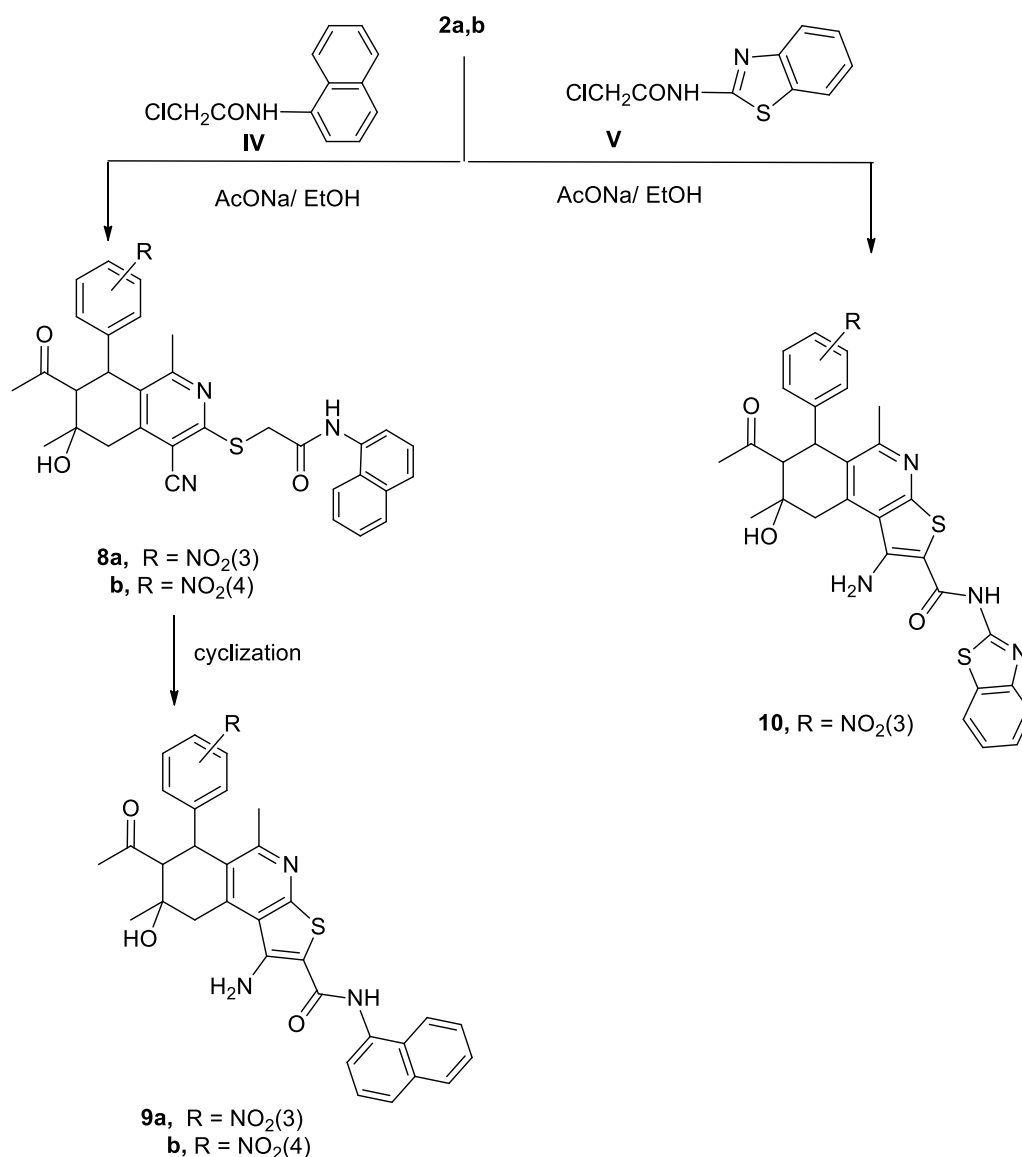
Scheme 1 Synthesis of compounds **2a–b**, **3–5**, **6a–c**, **7a–c**

compounds **2a–b** with the respective *N*-aryl-2-chloroacetamides **III(a–c)** in absolute ethanol in the presence of slightly excess molar amounts of sodium carbonate for 3 h (Scheme 1). Conversion of **6a–c** into the corresponding **7a–c** obeys intramolecular Thorpe-Ziegler cyclization.

In a similar manner, reaction of compound **2a–b** with *N*-(1-naphthyl)-2-chloroacetamide (**IV**) by refluxing in

ethanol, in the presence of slightly excess molar amounts of sodium acetate trihydrate, for one hour gave the corresponding *N*-(1-naphthyl)-(5,6,7,8-tetrahydroisoquinolin-3-ylthio)acetamides **8a, b** which can cyclized to **9a, b** (Scheme 2).

In contrast, reaction of **2a** with *N*-(benzthiazol-2-yl)-2-chloroacetamide (**V**) under the same (above) conditions yielded the cyclized form



Scheme 2 Synthesis of compounds **8a**, **8b**, **9a**, **9b** and **10**

1-amino-2-[(*N*-(benzthiazol-2-yl)]-6,7,8,9-tetrahydrothieno[2,3-*c*]isoquinoline-2-carboxamide **10** directly (Scheme 2).

The FT-IR, ^1H NMR, ^{13}C NMR spectra of all synthesized compounds were in agreement with the expected results (supplementary date S1–S42).

Cytotoxic activity

Compounds **3–5**, **12**, **2a**, **6a**, **7a**, **8a**, **8b** and **9b** were evaluated against nine human cancer cell lines at a single concentration point of 100 $\mu\text{g/ml}$ to determine their inhibitory efficacy. The cell lines are: (human liver carcinoma (**HEPG2** and **HUH7**), human breast carcinoma

(**MCF7**), colon carcinoma human (**HCT116** and **CACO2**), human lung carcinoma (**H460** and **A459**), human osteosarcoma (**MG-63**), normal human skin cell line (**HSF**) (Table 1, Fig. 1). According to the results in (Table 1, Fig. 1), all synthetic compounds are more targeted and have a lower percentage of inhabitation against the human skin cell line HSF than doxorubicin (positive control), indicating that they are safer for normal cell lines. The raw data can be found in supplementary Table (S1–S4), Figure (S43–S44).

Using the MTT test method, the *in vitro* cytotoxicity of our synthesized compounds at different doses ranging from 0 to 100 $\mu\text{g/ml}$ was examined in two cell lines,

Table 1 Inhibition activity in one spot 100 µg/ml concentration of all compounds against normal skin cell line HSF in compared with Doxorubicin

Compd.no	Inhibition percent of HSF cell line	Compd.no	Inhibition percent of HSF cell line
3	52	8a	59
4	50	8b	50
5	70	9b	58
10	56	Doxorubicin	60
2a	48		
6a	56		
7a	55		

HEPG2 and MCF7, to examine 50% of the cancer cells dying.

According to the results (Fig. 2, Table 2) two compounds, **3** and **2a**, showed the most potent cytotoxic activity against HEPG2, with IC₅₀ values of 75 and 82 g/ml, respectively when compared to the standard doxorubicin for the raw data, see (Table S3) in the accompanying information.

Also four compounds **8b**, **3**, **5** and **2a** exhibited significant cytotoxic action against MCF7, with corresponding IC₅₀ values of 12, 33, 33 and 35 g/ml (Fig. 3, Table 2). For the raw data in the supporting information (Table S4).

BY calculating the selectivity index (SI) of the synthesized compounds and Doxorubicin. $(SI) = IC_{50}$ of compound in normal cell lines / IC_{50} of the same compound in cancer cells [53, 54]. The synthesized compounds show selectivity index and the compounds **3**, **4**, **4**, **2a**, **6a** and **8b** showed SI > 2 when divided on MCF7 cell line that mean that this compounds safe and selective as anticancer drugs.

Cell cycle arrest of HEPG2 Cells

After adding compound **3**, we explore the growth inhibitory cell cycle mechanism of HEPG2 cell lines using DNA flow cytometry to examine the control and advancement of the cell cycle in HEPG2 cancer cells. Compound **3** was incubated with HEPG2 cells for 48 h at an IC₅₀ of 75 µg/ml. When compound **3** was applied to HEPG2 cells, the cells cycled between the G0-G1 and G2/M phases (Fig. 4, Table 3). The G2/M phase fraction increased from 12.12% (in control cells) to 25.67%. Compound **3** can also stop HEPG2 cells at the G0-G1% stage of the cell cycle, with an increase in the G0-G1phase fraction from 34.54 to 40.10.

Apoptosis induced

When compound **3** was applied to HEPG2 cells, early and late cellular apoptosis increased (from 0.20 to 13.45%) and (from 0.31 to 16.78%), respectively, according to the results of the Annexin V-FITC/PI assay. Showing a marked rise in overall apoptosis relative to the untreated control. Furthermore, (Table 4 and Figs. 5 and 6) show that the percentage of necrotic cells increased from 1.36 to 2.96%. HEPG2 cell death increases by 59 times following treatment with compounds **3**. Therefore compound **3** has a biological mechanism that inhibits the proliferation of HEPG2 cells and has cytotoxic effects against cancer.

Structure activity relationship (SAR)

The antiproliferate activity of tetrahydroisoquinoline is enhanced by its pyridine and benzene rings [31, 32, 43, 55–63]. Additionally, the three chiral centers in the synthesized compounds show the potential interaction with chiral biological molecules within cells, such as proteins, sugars, amino acids, enzymes, and nucleic acids [64–66]. The biomolecules can interact with the Asymmetric carbon centers with a variety of functional groups like acetyl, methyl, hydroxyl, cyano, amino in the cyclic form which found in our synthesized compounds. This interaction could result in biological activities such antioxidant, enzyme-inhibitory, and anticancer effects. Moreover, nitro groups allow for the formation of ionic connections with donor groups in the enzymes, which may enhance the biological activity [45–48]. Additionally, the synthesized compounds have high purity unless they three stereogenic centers, which means that each compound could have eight diastereomers. But due to the potential for hydrogen bonds between the acetyl and hydroxyl groups two chiral center cancel each other [49, 67–69]. According to the Structure–Activity Relationship (SAR) (Scheme 3) of the function group in the produced compounds and the anticancer activity, tetrahydroisoquinoline plays a significant role in biological activity [31, 32, 43, 55–60]. And the function groups were the mainly cause of biological activities. Compounds with carboxyl groups have been shown to exhibit anticancer properties against colon, breast, and lung cancer [70–72]. Methyl group-containing compounds are cytotoxic to lung, breast, and colon cancer cell lines [73]. Amino group-containing compounds show anticancer properties against lung and breast cancer [74]. Chlorine-containing compounds have anticancer effects on lung and breast cancer [75, 76]. Additionally, nitrile-group chemicals are cytotoxic to breast and lung cancer [77, 78]. Finally tetrahydroisoquinoline containing naphthyl groups are cytotoxic to liver, breast, and lung cancers [70, 79, 80].

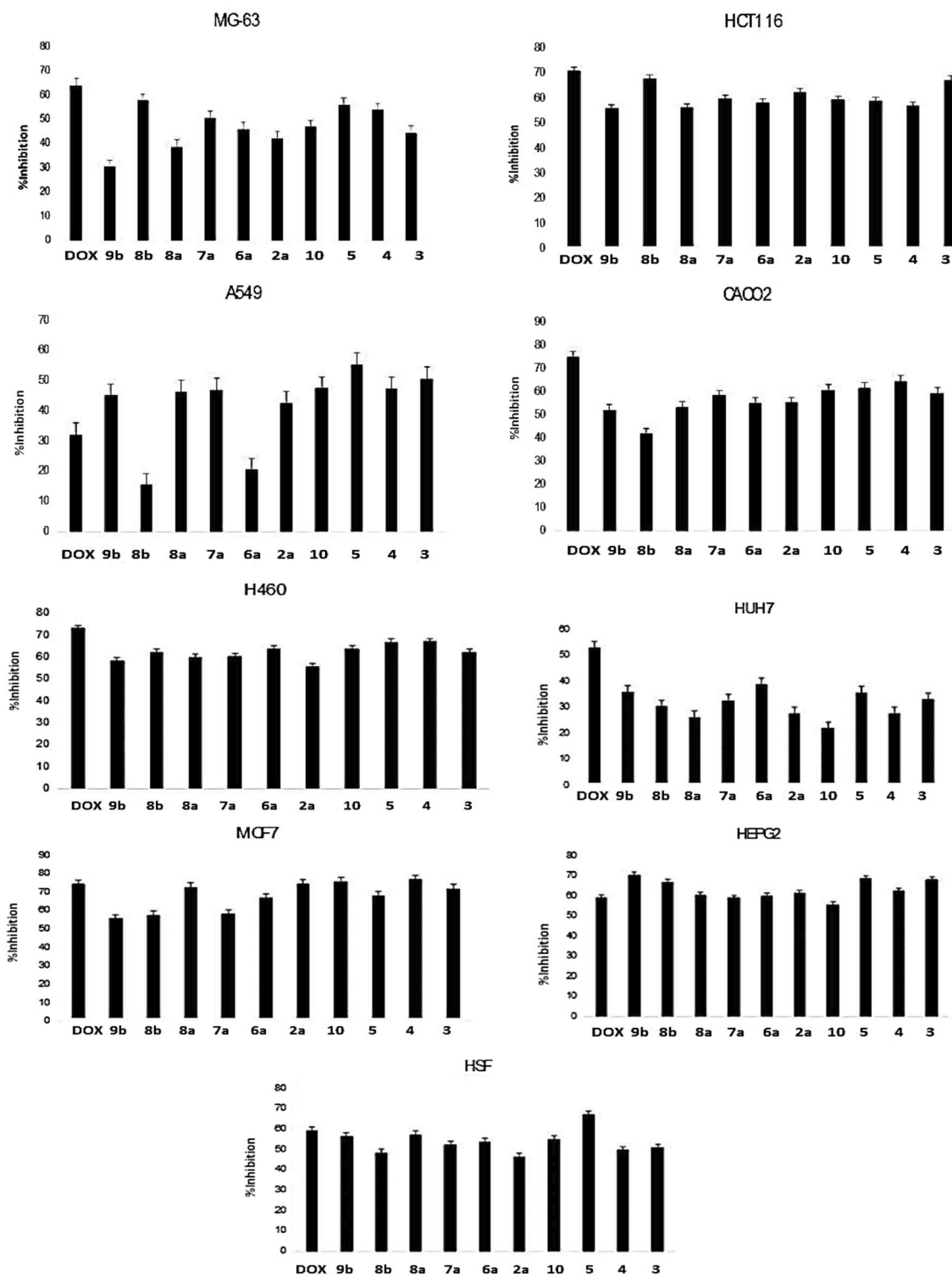


Fig. 1 Cytotoxicity for one spot concentration 100 µg/ml of the synthesized compounds against nine cell lines

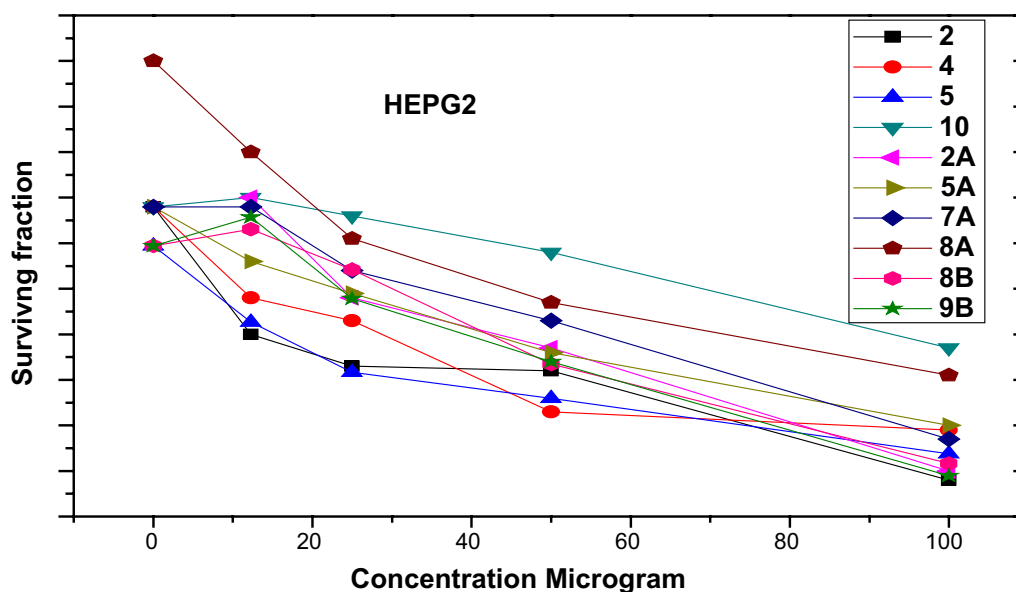


Fig. 2 Surviving fraction of HEPG2 cell lines after treatment by the synthesized compounds

Table 2 IC₅₀ of the synthesized compounds against MCF7 and HEPG2 cell lines and their selectivity index

Compd.no	IC ₅₀ FOR HSF ± S.D. µg/ml	IC ₅₀ for MCF7 ± S.D µg/ml	Selectivity Index = IC ₅₀ of HSF/ IC ₅₀ of MCF7	IC ₅₀ for HEPG2 ± S.D µg/ml	Selectivity Index = IC ₅₀ of HSF/ IC ₅₀ of HEPG2
3	96	33 ± 0.034	2.9	75 ± 0.063	1.2
4	100	47 ± 0.055	2.1	80 ± 0.070	1.2
5	71	33 ± 0.042	2.1	97 ± 0.053	0.73
10	89	> 100	–	> 100	–
2A	100	35 ± 0.061	2.8	82 ± 0.054	1.2
6A	89	21 ± 0.057	4.2	> 100	–
7A	90	50 ± 0.031	1.8	97 ± 0.054	0.92
8A	84	50 ± 0.019	1.6	88 ± 0.072	0.95
8B	100	12 ± 0.056	8.3	94 ± 0.82	1.1
9B	86	80 ± 0.050	1.1	87 ± 0.61	0.98
DOX	83	4.58 ± 0.081	18.1	4.13 ± 0.054	20.1

Molecular docking of the synthesized compounds binding with RET, HSP90 enzymes

Molecular docking experiments were done in I Mole Lab for Bioinformatics in Cairo, Egypt. Table 5 displays the results of the molecular docking on the various ligand (compound) binding affinities with the RET enzyme (Rearranged during Transfection) was provided by the results. Because it participates in cell signaling pathways that are critical for cell growth, differentiation, and survival RET a tyrosine kinase receptor, is important for antiprolifate. Given that RET is linked to several cancers, including thyroid cancer and several forms of lung cancer, the biological activity

of these compounds **8b** as potential RET inhibitors is very noteworthy. The ligand–protein interactions are numerically represented by the Gibbs free energy (ΔG) for compound **8b** (–6.8 kcal/mol). Values of the docking simulations; bigger negative values indicate higher binding. Compound **8b** demonstrated encouraging outcomes, forms a carbon hydrogen bond with, PRO892, Pi-sigma bond with VAL892, Pi-alkyl bond with ARG889, PRO931 and conventional hydrogen bond with LYS893 (Figs. 7, 8, Table 5). In comparison with the standard compound (alectinib) (ΔG) for compound **8b** (–7.2 kcal/mol).exhibits interactions, primarily relying on a carbon-hydrogen bond and hydrophobic

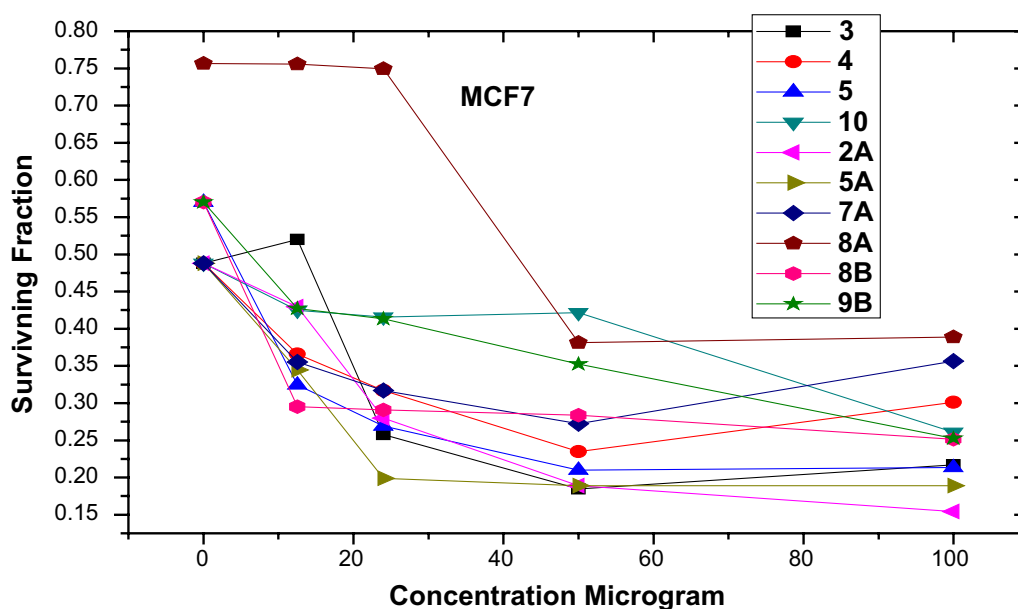


Fig. 3 Surviving fraction of MCF7 cell lines after treatment by the synthesized compounds

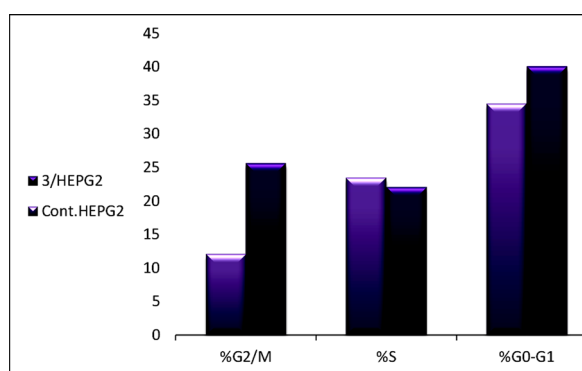


Fig. 4 Cell cycle analysis of HEPG2 treated with compound 3

Table 3 Cell cycle analysis of HEPG2 treated with compound 3

Code	%G0–G1	%S	%G2/M
3/HEPG2	40.1	22.10	25.67
Cont.HEPG2	34.54	23.51	12.12

Table 4 Apoptosis/necrosis assessment of HEPG2 cells after treatment with compounds 3

Code	Apoptosis			Necrosis
	Total	Early	Late	
3/HEPG2	33.19	13.45	16.78	2.96
Cont.HEPG2	1.87	0.2	0.31	1.36

interactions (Fig. 8) for more details see the supplementary information (Table S5, S6).

The strong binding affinities observed, especially for compound **8b** suggest that these ligands may effectively inhibit RET kinase activity by occupying its ATP-binding site or inducing conformational changes that prevent kinase activation. This inhibition could potentially disrupt the aberrant signaling cascades associated with RET enzyme driven cancers.

In conclusion, this molecular docking study has identified several promising lead compounds, particularly compound **8b** which demonstrate strong binding affinities to the RET tyrosine kinase receptor. These findings provide a solid foundation for further optimization and development of potent RET inhibitors, potentially leading to new therapeutic options for RET-associated malignancies.

Also the molecular docking study for compound **3** was performed in (I Mole Lab for Bioinformatics-Cairo-Egypt) tested for binding with heat shock protein (HSP90) and the result showed that our tested compound **3** exhibited promising binding affinity to HSP90, with a binding energy (ΔG) of -6.8 kcal/mol, which is comparable to the standard Onalespib (-7.1 kcal/mol). This relatively small difference of 0.3 kcal/mol suggests that our tested compound could potentially serve as an effective HSP90 inhibitor, though slightly less potent than Onalespib (Table 6, Figs. 9, 10).

The detailed interaction analysis revealed that our tested compound **3** forms a complex network of interactions with HSP90, including three conventional hydrogen bonds with TYR305 and ARG378 residues, with

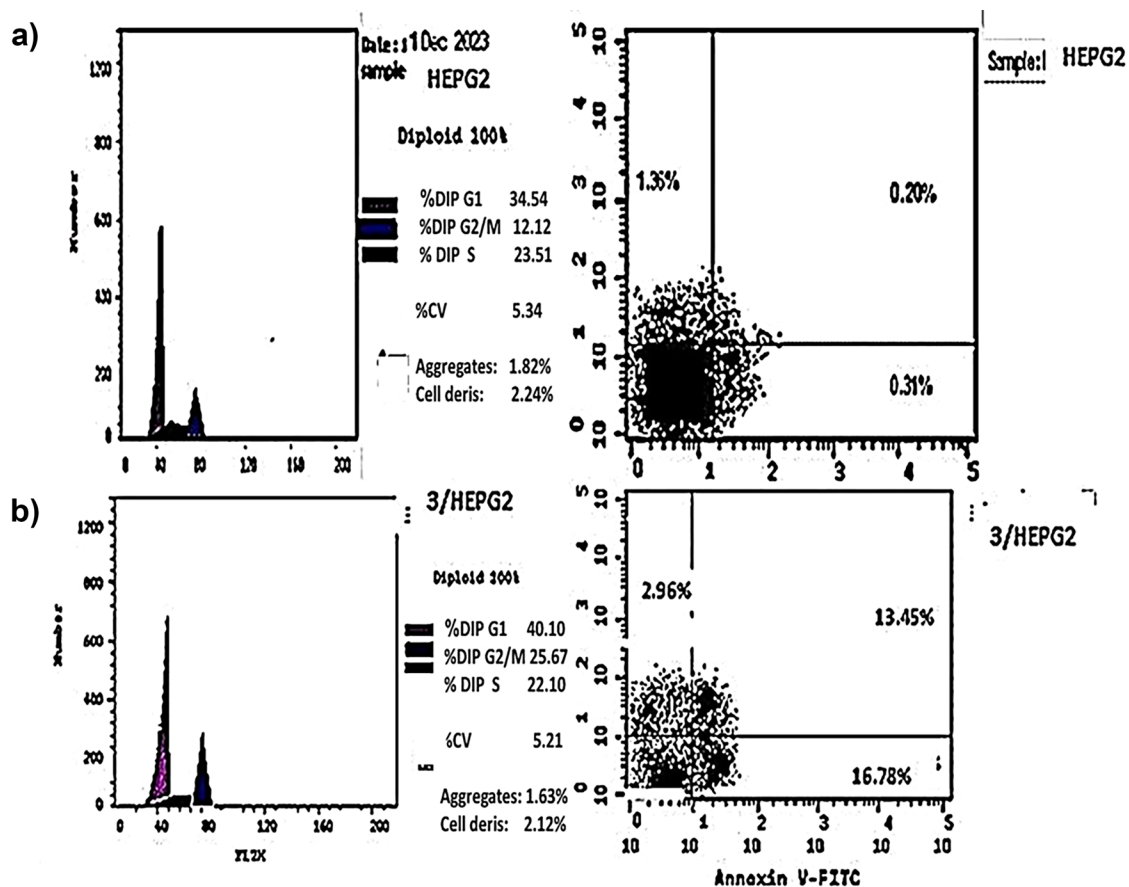


Fig. 5 Apoptosis of HEPG2 after treatment with compounds **3**. **a** Control HEPG2. **b** Compound **3**/HEPG2

distances ranging from 2.41 to 2.71 Å. These hydrogen bonds likely contribute significantly to the stability of the protein–ligand complex. The presence of a pi-anion interaction with ASP311 (4.04 Å) and a pi-sulfur interaction with PHE341 (5.27 Å) further strengthens the binding. Additionally, the compound forms hydrophobic interactions through pi-pi T-shaped and pi-alkyl interactions with PHE341, which are crucial for maintaining the proper orientation of the ligand within the binding pocket) for more details see the supplementary information (Tables S7, S8).

In contrast, the standered (Onalespib) showed a different interaction pattern, primarily forming a carbon hydrogen bond with ASP364 and a pi-cation interaction with ARG378. This distinct interaction profile, despite resulting in a slightly better binding energy, suggests that our tested compound **3** might offer unique advantages through its more diverse interaction network.

The biological implications of these findings are particularly noteworthy. HSP90 plays a crucial role in protein folding and stability, and its inhibition has been widely studied as a therapeutic strategy in various

diseases, particularly cancer. The strong binding affinity and multiple interaction points observed with our tested compound **3** suggest it could effectively disrupt HSP90 function. The involvement of TYR305 and ARG378 in hydrogen bonding is especially significant, as these residues are known to be important for HSP90's chaperoning function.

From a toxicological perspective, the binding energy and interaction profile suggest that our compound **3** might have a favorable safety profile. The presence of multiple, specific interactions, rather than random binding, indicates selective targeting of HSP90. This specificity is crucial for minimizing off-target effects and potential toxicity. The similar binding energy to Onalespib, an established HSP90 inhibitor with known safety parameters, provides additional confidence in the potential safety profile of our tested compound.

These molecular docking results complete an important piece of the drug development puzzle by providing detailed structural insights into how our compound interacts with its target. The combination of favorable binding energy and specific molecular interactions

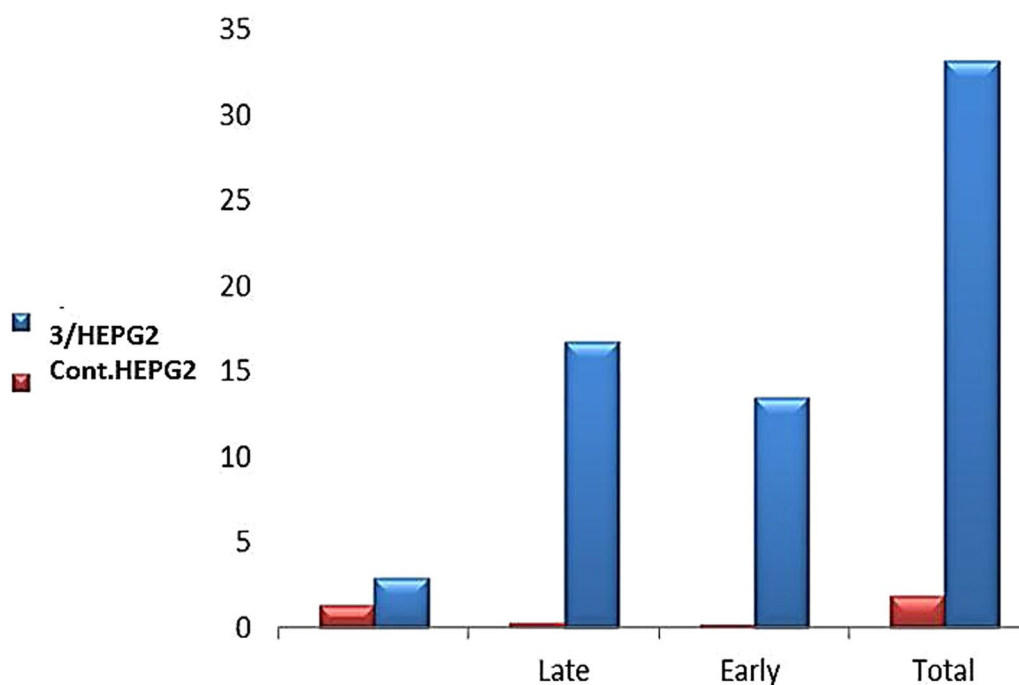


Fig. 6 Apoptosis/necrosis assessment of HEPG2 cells after treatment with compounds

suggests that our tested compound could be a viable candidate for further development as an HSP90 inhibitor. However, these computational findings should be validated through experimental studies to confirm the predicted binding mode and biological activity.

Experimental

Instrumentations

Instruments which used to measure the analysis of our synthesized compounds like melting point and ^1H NMR, ^{13}C NMR, FT-IR, Mass spectroscopy and elemental analysis were the same used in our pervious work [50–52].

Reaction of 2-acetylcyclohexanones 1a-b with cyanothioacetamide; synthesis of compounds 2a-b; general method

The general procedure for synthesis the starting material 2a, b was mentioned before in our pervious published papers [50–52].

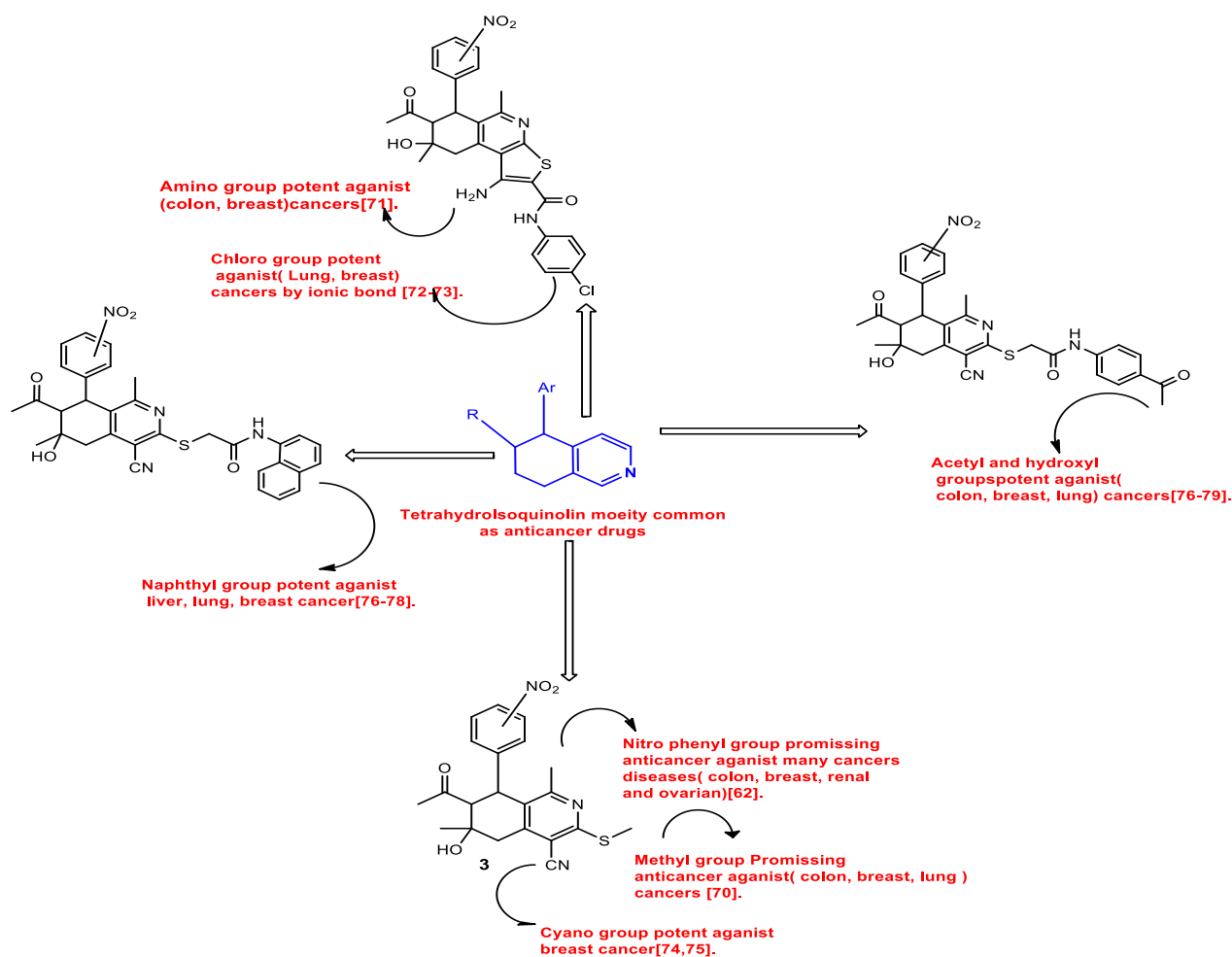
7-Acetyl-4-cyano-1,6-dimethyl-6-hydroxy-8-(3-nitrophenyl)-5,6,7,8-tetra-hydroisoquinoline-3(2H)-thione (2a)

It is synthesized by reaction of 1a with cyanothioacetamide Yield: 96%; m. p: 279–280 °C. Color: yellow to orange crystals. Recrystallized from ethanol. The FT-IR spectrum of compound 2a show characteristics band at: 3429 cm^{-1} for (O–H), 3230 cm^{-1} for (N–H); 3139 cm^{-1} for (C–H, sp^2); 2971 cm^{-1} for (C–H, sp^3); 2221 cm^{-1} for (C \equiv N); 1710 cm^{-1} for (C=O). ^1H NMR spectrum of

compound 2a (500 MHz, DMSO- d_6) show signals at δ : 13.68 (s, 1H, NH); 7.95–8.05 (m, 2H, ArH); 7.51–7.58 (m, 2H, ArH); 5.05 (s, 1H, OH); 4.61–4.63 (d, $J=10$ Hz, 1H, C 8 H); 3.23–3.26 (d, $J=15$ Hz, 1H, C 5 H), 2.88–2.90 (d, $J=10$ Hz, 1H, C 7 H), 2.83–2.87 (d, $J=20$ Hz, 1H, C 5 H); 2.12 (s, 3H, COCH $_3$); 1.84–1.86 (d, $J=10$ Hz, 3H, CH $_3$); 1.23 (s, 3H, CH $_3$). Anal. calcd for C $_{20}$ H $_{19}$ N $_3$ O $_4$ S (397.11): C, 60.44; H, 4.82; N, 10.57%. Found: C, 60.67; H, 5.11; N, 10.28%

7-Acetyl-4-cyano-1,6-dimethyl-6-hydroxy-8-(4-nitrophenyl)-5,6,7,8-tetra-hydroisoquinoline-3(2H)-thione (2b)

It is synthesized by reaction of 1b with cyanothioacetamide Yield: 93%; m. p 290–291 °C. The FT-IR spectrum of compound 2b show characteristics band at: 3482 cm^{-1} for (O–H); 3235 cm^{-1} for (NH); 3106 cm^{-1} for (C–H, sp^2); 2971, 2872 cm^{-1} for (C–H, sp^3); 2220 cm^{-1} for (C \equiv N); 1708 cm^{-1} for (C=O). ^1H NMR spectrum of compound 2b in (500 MHz, DMSO- d_6) show signals at δ : 13.85(S, H, NH) 7.84–7.86 (d, $J=10$ Hz, H, ArH); 7.62–7.64 (d, $J=10$, H, ArH); 7.51–7.53 (d, $J=10$ Hz, H, ArH); 7.33–7.34 (d, $J=5$ Hz, H, Ar), 5.04 (s, 1H, OH); 4.97–4.99 (d, $J=10$ Hz, 1H, C 8 H); 3.33 (s, 1H, C 5 H);, 3.16–3.10 (m, 1H, C 7 H), 2.86–2.90 (d, $J=20$ Hz, 1H, C 5 H); 2.02 (s, 3H, COCH $_3$); 1.93 (s, 3H, CH $_3$); 1.29 (s, 3H, CH $_3$). Anal. calcd for C $_{20}$ H $_{19}$ N $_3$ O $_4$ S (397.11): C, 60.44; H, 4.82; N, 10.57%. Found: C, 60.32; H, 5.04; N, 10.33%.



Scheme 3 SAR study of interaction position of tetrahydroisoquinoline derivatives

Reaction of compounds **2a–b** with methyl iodide, ethyl chloroacetate, chloroacetonitrile or its *N*-aryl-2-chloroacetamides **III(a–c)**, **IV**; Synthesis of compounds **3–5**, **6a–c** and **8a,b** general method (A) were carrying according to the general method in our previous work [50–52]

A mixture of **2a–b** (10 mmol), a halocompound (10 mmol) was refluxed in ethanol in the presence of sodium acetate trihydrate (1.50 g, 11 mmol). The formed solid that were cooling and collected to recrystallized from ethanol to give crystals of compounds **3–5**, **6a–c**.

7-Acetyl-4-cyano-1,6-dimethyl-6-hydroxy-3-methylthio-8-(3-nitrophenyl)-5,6,7,8-tetrahydroisoquinoline (3)

It is synthesized by reaction of **2a** with methyl iodide. Yield: 94%; 150 m.p.: 149–150 °C. The FT-IR spectrum of compound **3**: 3500 cm^{-1} for (O–H); 3077 cm^{-1} for (C–H, sp^2); 2971–2931 cm^{-1} for (C–H, sp^3); 2213 cm^{-1} for (C \equiv N); 1701 cm^{-1} for (C=O acetyl). ^1H NMR spectrum of compound **3** in (400 MHz, DMSO- d_6) show signals at δ : 7.95–8.09 (m, 2H, ArH); 7.55–7.59 (m, 2H, ArH); –4.98 (s, 1H, OH), 4.77–4.79 (d, $J=8$ Hz, 1H, C 8 H), 3.21–3.36 (m, 3H, CH $_3$), 3.13–3.15 (t, $J=8$ Hz, 1H, C 7 H); 2.87–2.95 (m, 2 H, 2C 5 H); 2.18 (s, 3H, COCH $_3$), 1.98 (s, 3H, CH $_3$); 1.27–1.29 (s, 3H, CH $_3$). ^{13}C NMR δ 208.96, 160.66, 158.33, 150.10, 147.96, 146.09, 135.17, 130.18, 128.28, 122.69, 121.73, 115.18, 104.50, 67.40, 65.96, 43.27, 42.9, 31.04, 27.54, 24.90, 23.79, 14.49. Anal. calcd for C $_{21}$ H $_{21}$ N $_3$ O $_4$ S (411.13): C, 61.30; H, 5.14; N, 10.21. found C, 62.18; H, 5.44; N, 10.00.

Table 5 ΔG (kcal/mol) for each ligand with protein (RET)

Ligand	ΔG (kcal/mol)
Compound 8b	–6.8
Standard (alectinib)	–7.2

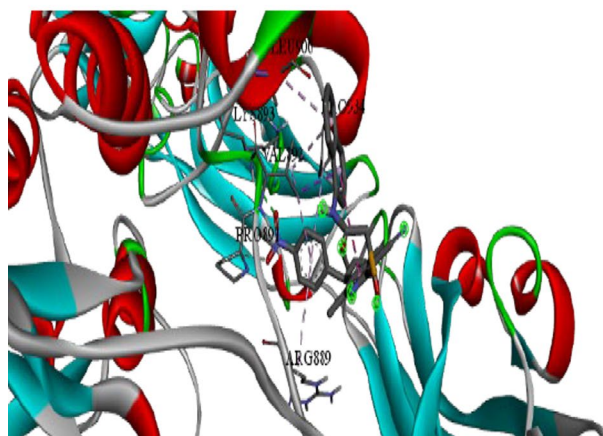


Fig. 7 3D, 2D Molecular Docking of compound **8b** with RET receptor

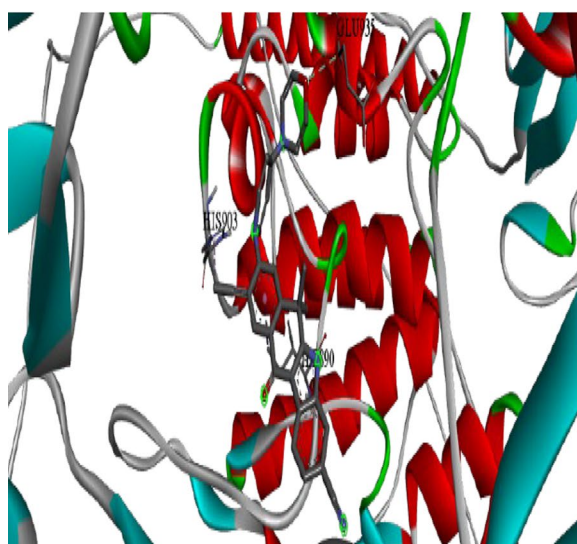
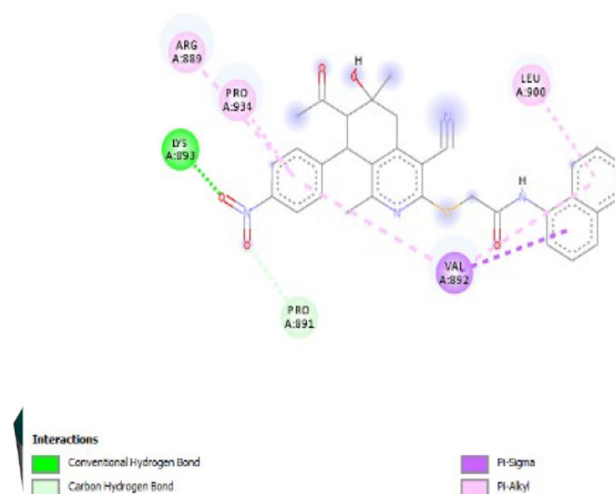


Fig. 8 3D, 2D Molecular Docking of standard (alectinib) with RET receptor

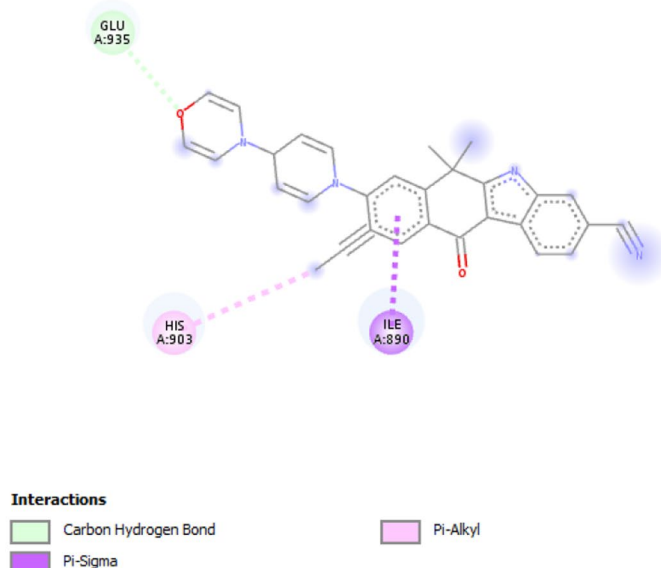


Table 6 ΔG (kcal/mol) and binding affinity for each compounds 3 tested with protein

compound	ΔG (kcal/mol)
Standard (Onalespib)	-7.1
Compound 3	-6.8

Ethyl 2-[(7-acetyl-4-cyano-1,6-dimethyl-6-hydroxy-8-(3-nitrophenyl)-5,6,7,8-tetra-hydroisoquinolin-3-yl)thio]acetate (4)

It is synthesized by reaction of **2a** with ethylchloroacetate Yield:93%; m.p.: 177–180 °C. The FT-IR spectrum

of compound **4**: 3495 cm^{-1} (O–H); 3079 cm^{-1} (C–H, sp^2); 2984–2933 cm^{-1} (C–H, sp^3); 2217 cm^{-1} ($\text{C}\equiv\text{N}$); 1723, 1700 cm^{-1} (C=O ester, acetyl). ^1H NMR spectrum of compound **4** in (400 MHz, DMSO- d_6) show signals at δ : 8.12–8.14 (m, 1H, ArH); 7.8 (s, 1H, ArH); 7.50–7.54 (t, $J=16$ Hz, 1H, ArH); 7.35–7.36 (d, $J=4$ Hz, 1H, ArH); 4.50–4.52 (d, $J=8$ Hz 1H, OH), 4.11–4.14 (m, 2H, CH_2 acetate), 3.91 (s, 6.8 Hz, 2H, C^8 H, C^5 H), 2.98–3.18 (m, 5.5 Hz, 4H, SCH_2 , C^7 H, C^5 H); 1.85–1.88 (d, $J=12$ Hz, 6H, CH_3 , COCH_3), 1.38 (s, 3H, CH_3); 1.2 (s, 3H, CH_3).

The mass spectrum show molecular ion peak at m/z $[M^+]=483.11$ in agreement with its molecular formula:

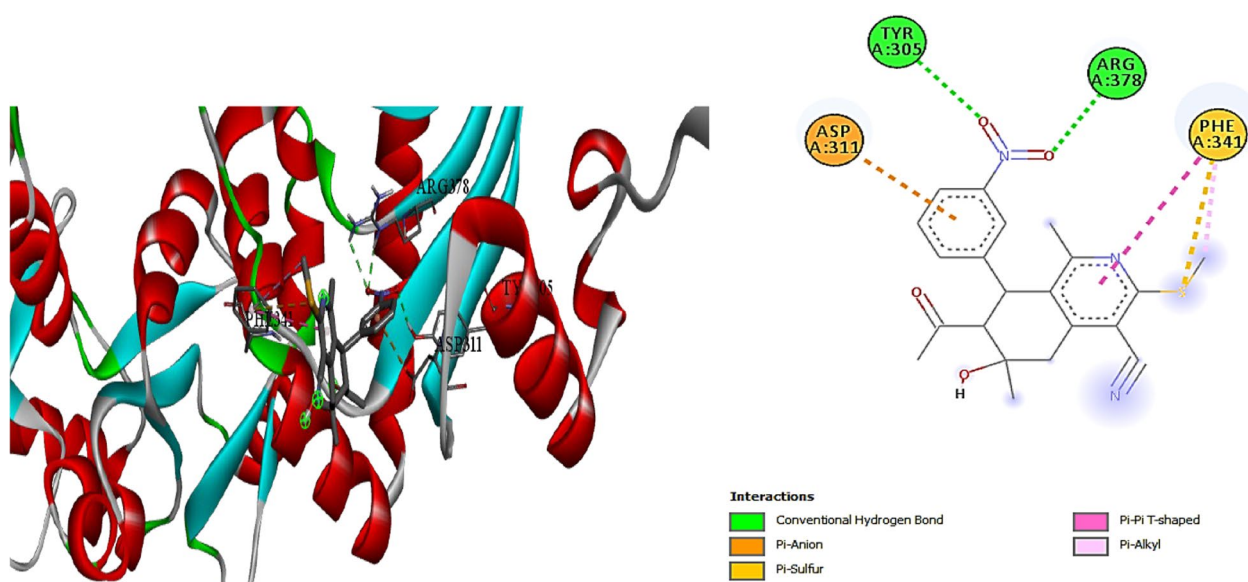


Fig. 9 3D, 2D Molecular Docking of compound **3** with HSP90 protein

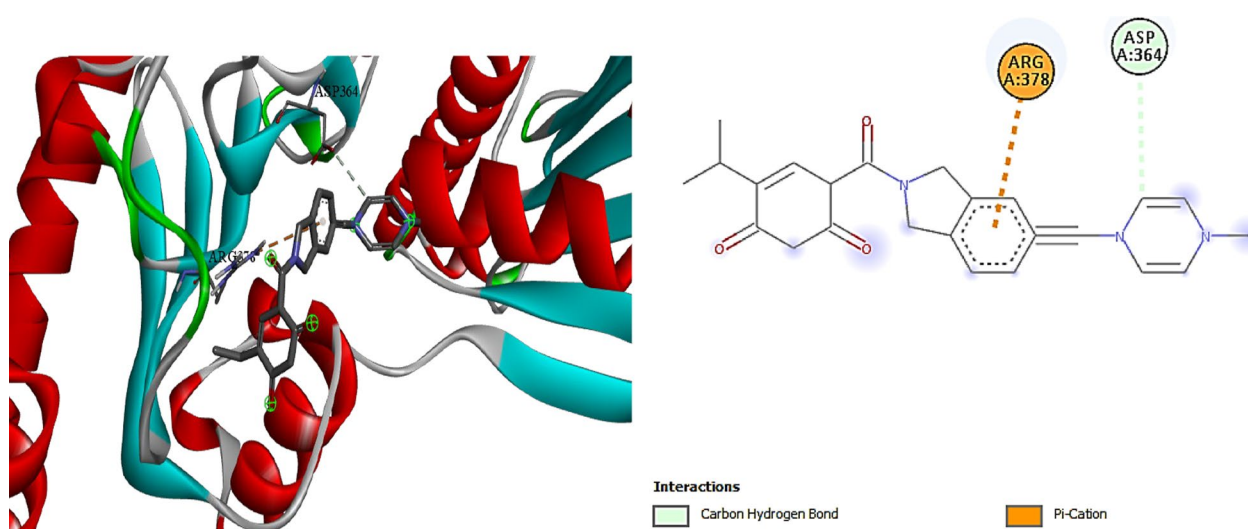


Fig. 10 3D, 2D Molecular Docking of Standard ligand (Onalespib) and protein HSP90

($C_{24}H_{25}N_3O_6S$) with the exact mass: 483.15. The most abundant peak (base peak) at 439 due to cleavage of ester group and form the aldehyde ($C_{22}H_{22}N_3O_5S$). Anal. calcd for $C_{24}H_{27}N_3O_6S$ (485.16): C, 59.37; H, 5.60; N, 8.65 found C, 59.59; H, 5.20; N, 8.75.

2-[(7-Acetyl-4-cyano-1,6-dimethyl-6-hydroxy-8-(4-nitrophenyl)-5,6,7,8-tetra-hydroisoquinolin-3-yl)thio]acetoneitrile (5**)**

It is synthesized by reaction of **2b** with chloroacetonitrile. Yield: 90%; m.p.: 183–185 °C. The FT-IR spectrum of compound **5**: 3508 cm^{-1} for (O–H); 3108 cm^{-1} for (C–H,

sp^2); 2972, 2931 cm^{-1} for (C–H, sp^3); 2250, 2216 cm^{-1} for ($2C\equiv N$); 1701 cm^{-1} for (C=O, acetyl). 1H NMR spectrum of compound **5** in (400 MHz, DMSO- d_6) show signals at δ δ : 8.14–8.16 (d, $J=8$ Hz, 2H, 2 Ar–H), 7.37–7.39 (d, $J=8$ Hz, 2H, 2Ar–H), 4.98 (s, 1H, OH), 4.80 (s, 1H, C^8H), 4.28–4.33 (m, 2H, SCH_2), 3.32–3.36 (s, 1H, C^5H), 2.92–2.99 (t, $J=12$ Hz, 2H, C^7H , C^5H); 2.19 (d, 3H, $COCH_3$), 2.05 (s, 3H, CH_3); 1.31 (s, 3H, CH_3). ^{13}C NMR spectrum of compound **5** (DMSO- d_6) show environments of carbon as expected at δ : 209.08, 161.57, 155.28, 152.02, 151.10, 146.70, 130.07, 124.33, 118.02, 115.02, 106.8, 105, 67.95,

66.18, 56.52, 43.28, 40.66, 31.65, 27.97, 25.04, 18.98, 15.82. Anal. calcd for $C_{21}H_{18}N_4O_4S$ (422.10): C, 59.70; H, 4.29; N, 13.26. Found C, 59.55; H, 4.30; N, 12.1%.

2-[(7-Acetyl-4-cyano-1,6-dimethyl-6-hydroxy-8-(3-nitrophenyl)-5,6,7,8-tetra-hydroisoquinolin-3-yl)thio]-N-(4-acetylphenyl)acetamide (6a)

It was synthesized by reaction of **2a** with *N*-(4-acetylphenyl)-2-chloroacetamide. Yield: 93%; m.p.:231–232 °C. The FT-IR spectrum of compound **6a**: 3420 cm^{-1} (O–H); 3344 cm^{-1} (N–H); 2970 cm^{-1} (C–H, sp^2); 2925 cm^{-1} (C–H, sp^3); 2217 cm^{-1} (C≡N); 1702, 1674 cm^{-1} (C=Oamide, C=O acetyl). 1H NMR spectrum of compound **6a** in (400 MHz, DMSO- d_6) show signals at δ : 10.56 (s, 1H, NH), 7.50–8.05 (m, 8H, 8ArH), 4.97 (s, 1H, OH), 4.73–4.75 (d, $J=8$ Hz, 1H, C^8H), 4.10–4.18 (m, 2H, SCH_2), 3.31 (s, 1H, C^5H) 2.87–2.95 (t, $J=8$ Hz, 2H, C^7H and C^5H), 2.49 (s, 3H, $COCH_3$), 2.15 (s, 3H, $COCH_3$), 1.85 (s, 3H, CH_3 attached to pyridine ring), 1.26 (s, 3H, CH_3). ^{13}C NMR spectrum of compound **6a** (DMSO- d_6) show 27 environments of carbon as expected at δ 208.87, 196.18, 166.72, 160.49, 157.53, 150.23, 147.90, 145.96, 143.20, 135.12, 131.71, 130.15, 129.43, 128.70, 122.68, 121.70, 118.19, 115.02, 104.02, 67.53, 66.00, 43.26, 42.40, 34.85, 30.96, 27.47, 26.32, 24.57. Anal. Calcd. for $C_{30}H_{28}N_4O_6S$ (572.17): C, 62.92; H, 4.93; N, 9.78%. Found: C, 62.95; H, 5.09; N, 9.75%.

2-[(7-Acetyl-4-cyano-1,6-dimethyl-6-hydroxy-8-(4-nitrophenyl)-5,6,7,8-tetra-hydroisoquinolin-3-yl)thio]-N-(4-acetylphenyl)acetamide (6b)

It was synthesized by reaction of **2b** with *N*-(4-acetylphenyl)-2-chloroacetamide. Yield: 86%. M.p. 193–194 °C. The FT-IR spectrum of compound **6b**: 3540 cm^{-1} for (O–H); 3337 cm^{-1} for (N–H); 3109 cm^{-1} for (C–H, sp^2); 2968 cm^{-1} for (C–H, sp^3); 2220 cm^{-1} for (C≡N); 1683 cm^{-1} for (C=Oacetyl and amide), 1595 for (C=N). 1H NMR spectrum of compound **6b** in (400 MHz, DMSO- d_6) show signals at δ : 10.57 (s, 1H, NH), 8.06–8.11 (d, $J=25$ Hz, 2H, ArH), 7.84 (d, $J=10$ Hz, 2H, ArH), 7.62– (s, ArH), 7.28–7.31 (d, $J=15$ Hz, 2H, ArH), 5.02 (s, 1H, OH), 4.67–4.78 (s, 1H, C^8H), 4.34 (s, 1H, C^5H), 4.11 (s, 2H, SCH_2), 2.88–2.89 (d, $J=5$ Hz, 2H: C^7H and C^5H), 2.12 (s, 3H, $COCH_3$), 1.80 (s, 3H, $COCH_3$), 1.23 (s, 3H, CH_3 attached to pyridine ring), 1.03 (s, 3H, CH_3). Anal. Calcd for $C_{30}H_{28}N_4O_6S$ (572.17): C, 62.92; H, 4.93; N, 9.78. Found: C, 63.00; H, 4.85; N, 10.06.

2-[(7-Acetyl-4-cyano-1,6-dimethyl-6-hydroxy-8-(4-nitrophenyl)-5,6,7,8-tetra-hydroisoquinolin-3-yl)thio]-N-(4-chlorophenyl)acetamide (6c)

It was synthesized by reaction of **2b** with *N*-(4-chlorophenyl)-2-chloroacetamide Yield: 94%; m.p.:

144–145 °C. The FT-IR spectrum of compound **6c**: 3563 cm^{-1} for (O–H), 3344 cm^{-1} for (N–H); 3203 cm^{-1} for (C–H, sp^2); 2972, 2937 cm^{-1} for (C–H, sp^3); 2221 cm^{-1} for (C≡N); 1705 cm^{-1} for (C=O, acetyl); 1681 cm^{-1} for (C=O, amide). 1H NMR spectrum of compound **6c** in (400 MHz, DMSO- d_6) show signals at δ : 10.35 (s, 1H, NH), 8.08–8.11 (m, 2H, ArH), 7.60–7.62 (d, $J=8$ Hz, 2H, ArH), 7.29–7.54 (m, 4H, ArH), 4.98 (s, 1H, OH), 4.71–4.73 (d, $J=8$ Hz, 1H, CH at C^8), 4.06–4.14 (dd, $J=12,12$ Hz, 2H, SCH_2), 3.42–3.44 (d, $J=8$ Hz, 1H, C^5H), 2.90–2.92 (t, $J=10$ Hz, 2H: C^7H and C^5H), 2.15(s, 3H, $COCH_3$), 1.85 (s, 3H, CH_3), 1.27 (s, 3H, CH_3). ^{13}C NMR spectrum of compound **6c** (DMSO- d_6) show 28 environments of carbon as expected at δ : 208.53, 166.23, 164.75, 160.47, 157.63, 151.75, 150.04, 146.07, 137.85, 129.52, 128.73, 128.60, 126.83, 123.77, 120.90, 120.53, 114.98, 103.98, 67.39, 65.71, 55.99, 43.21, 42.65, 34.72, 31.02, 27.46, 24.45, 18.50. Anal. Calcd. for $C_{28}H_{25}ClN_4O_5S$ (564.12): C, 59.52; H, 4.46; N, 9.92%. Found: C, 59.20; H, 4.67; N, 10.07%.

Synthesis of 7-Acetyl-1-amino-2-(N-arylcarbamoyl)-5,8-dimethyl-8-hydroxy-6-(3-nitrophenyl or 4-nitrophenyl)-6,7,8,9-tetrahydrothieno[2,3-c]isoquinolines compounds 7a-c, 9a,b and 10 general method (B).

To a suspension of **6a–c**, **8a**, **b** (10 mmol) were refluxed in absolute ethanol (60 mL) using sodium carbonate for 3 h. The yellow solid that formed and recrystallized from ethanol to give **7a–c** according to the procedure in the pervious work [50–52].

7-Acetyl-N-(4-acetylphenyl)-1-amino-5,8-dimethyl-8-hydroxy-6-(3-nitro-phenyl)-6,7,8,9-tetrahydrothieno[2,3-c]isoquinoline-2-carboxamide (7a)

It was obtained by cyclization of compound **6a** Yield: 90%; m.p.:277–280 °C. The FT-IR spectrum of compound **7a**: 3416, 3316 cm^{-1} for (O–H, NH_2 , NH); 2967, 2917 cm^{-1} for (C–H, sp^3); 1701 cm^{-1} for (C=O). 1H NMR spectrum of compound **7a** in (400 MHz, DMSO- d_6) show signals at δ : 9.73 (s, 1H, NH), 8.30 (s, 1H, Ar–H), 7.84–8.08 (m, 6H, 6Ar–H), 7.52–7.58 (m, 2H, NH_2), 7.20 (s, 1H, Ar–H), 4.86–4.88(d, $J=8$ Hz, 2H, OH, C^6H), 3.65–3.68 (s, 1H, C^9H), 3.39–3.42 (d, $J=12$ Hz, 1H, C^7H), 2.93–2.95 (d, $J=8$ Hz, 1H, C^9H), 2.55 (s, 3H $COCH_3$), 2.20 (s, 3H, $COCH_3$), 2.03 (s, 3H, CH_3), 1.33 (s, 3H, CH_3). ^{13}C NMR spectrum of compound **7a** (DMSO- d_6) show 25 environments of carbon as expected at δ : 209.43, 196.56, 164.35, 158.59, 156.80, 150.17, 147.93, 147.01, 143.60, 143.07, 135.50, 131.12, 130.12, 129.06, 125.35, 122.81, 122.43, 121.54, 119.93, 96.44, 79.14, 44.28, 42.89, 42.03, 31.17, 28.95, 27.93, 26.44, 24.77, 24.47, 22.08.

Anal. Calcd. for $C_{30}H_{28}N_4O_6S$ (572.17): C, 62.92; H, 4.93; N, 9.78%. Found: C, 62.87; H, 5.29; N, 9.88%.

7-Acetyl-N-(4-acetylophenyl)-1-amino-5,8-dimethyl-8-hydroxy-6-(4-nitro-phenyl)-6,7,8,9-tetrahydrothieno[2,3-c]isoquinoline-2-carboxamide (7b)

It was obtained by cyclization of compound **6b**. Yield: 89%; m.p.: 301–302 °C. IR; The FT-IR spectrum of compound **7b**: 3422, 3322 cm^{-1} for (O–H, NH₂, NH); 2918 cm^{-1} for (C–H, sp³); 1702, 1679 cm^{-1} for (2 acetyl C=O). ¹H NMR spectrum of compound **7b** in (400 MHz, DMSO-d₆) show signals at δ : 9.71 (s, 1H, NH), 8.11–8.14 (t, $j=12$ Hz, 3H, 3 Ar–H), 7.83–7.91 (m, 4H, 4Ar–H), 7.16–7.20 (m, 3H, Ar–H, NH₂), 4.82–4.84(d, $J=8$ Hz, 1H, OH), 3.59–3.70 (s, 1H, C⁹H), 3.40–3.52 (d, $J=12$ Hz, 2H, C⁶H, C⁷H), 2.86–2.89 (d, $J=8$ Hz, 1H, C⁹H), 2.52–2.58 (s, 3H COCH₃), 2.45 (s, 3H, CO CH₃), 1.99–2.00 (s, 3H, CH₃), 1.30 (s, 3H, CH₃). ¹³C NMR spectrum of compound **7b** (DMSO-d₆) show 21 environments of carbon as expected at δ : ¹³C NMR δ : 209.17, 169.80, 156.77, 153.03, 146.12, 132.10, 129.35, 129.02, 125.67, 123.78, 121.39, 120.13, 67.12, 66.11, 65.74, 43.17, 41.95, 31.17, 27.92, 26.35, 24.60. Anal. Calcd. for C₃₀H₂₈N₄O₆S (572.17): C, 62.92; H, 4.93; N, 9.78%. Found: C, 62.87; H, 5.29; N, 9.88%.

Anal. Calcd. for: C₃₂H₃₄N₄O₄S: (570.23): C, 67.35; H, 6.00; N, 9.82%. 200.42 Found: C, 67.51; H, 6.09; N, 9.74%.

7-Acetyl-1-amino-N-(4-chlorophenyl)-5,8-dimethyl-8-hydroxy-6-(3-nitrophenyl)-6,7,8,9-tetrahydrothieno[2,3-c]isoquinoline-2-carboxamide (7c)

It was obtained by reaction of **2a** with *N*-(4-chlorophenyl)-2-chloroacetamide in the presence of sodium carbonate. Yield: 94%; m.p.: 293–294 °C. Anal. The FT-IR spectrum of compound **7c**: 3417, 3383, 3314 cm^{-1} for (O–H, NH₂, N–H); 3095 cm^{-1} for (C–H, sp²); 2967, 2916 cm^{-1} for (C–H, sp³); 1706 cm^{-1} for (C=O, acetyl); 1622 cm^{-1} for (C=O, amide). ¹H NMR spectrum of compound **7c** in (400 MHz, DMSO-d₆) show signals at δ : 9.56 (s, 1H, NH), 8.06–8.08 (m, 1H, 1Ar–H), 7.74–7.84 (m, 3H, 3Ar–H), 7.57–7.58 (d, 2H, 2Ar–H), 7.51–7.55 (t, 2H, NH₂), 7.13–7.39 (m, 2H, Ar–H), 4.85–4.88(t, $J=12$ Hz, 2H, OH, C⁹H), 3.64–3.67 (s, 1H, C⁷H), 3.40–3.44 (d, $J=12$ Hz, 1H, C⁹H), 2.93–2.95 (d, $J=8$ Hz, 1H, C⁶H), 2.21 (s, 3H, CO CH₃), 2.04 (s, 3H, CH₃), 1.33 (s, 3H, CH₃). ¹³C NMR spectrum of compound **7c** (DMSO-d₆) show 25 environments of carbon as expected at δ : 209.42, 164.35, 158.33, 156.65, 149.62, 147.92, 147.04, 142.94, 135.07, 130.10, 128.27, 128.23, 126.96, 122.95, 122.65, 122.41, 121.51, 96.41, 67.14, 65.88, 42.8, 41.99, 31.17, 27.94, 24.74. Anal. Calcd. for C₂₈H₂₅ClN₄O₅S (564.12): C, 59.52; H, 4.46; N, 9.92%. Found: C, 59.3; H, 5.01; N, 9.90%.

2-[(7-Acetyl-4-cyano-1,6-dimethyl-6-hydroxy-8-(3-nitrophenyl)-5,6,7,8-tetrahydro-isoquinolin-3-yl)thio]-N-(naphthalen-1-yl)acetamide (8a)

It was obtained by reaction of compound **2a** with *N*-(1-naphthyl)-2-chloroacetamide (IV) Yield: 86%; m.p.: 237–238 °C. The FT-IR spectrum of compound **8a**: 3527 cm^{-1} for (O–H); 3401 cm^{-1} for (N–H); 3085 cm^{-1} for (C–H, sp²); 2970, 2928 cm^{-1} for (C–H, sp³); 2214 cm^{-1} for (C≡N); 1702 cm^{-1} for (C=O, acetyl); 1665 cm^{-1} for (C=O, amide) 0.1597 cm^{-1} for (C=N). ¹H NMR spectrum of compound **8a** in (400 MHz, DMSO-d₆) show signals at δ : 10.19 (s, 1H, NH); 7.37–8.08 (m, 11H, ArH); 5.00–5.01 (s, 1H, OH); 4.75–4.76 (d, $J=8$ Hz, 1H, C⁸H); 4.27 (d, 2H, SCH₂); 3.25–3.26 (d, $J=4$ Hz, 1H, C⁵H), 2.87–2.95 (m, 2H: C⁷H and C⁵H), 2.14–2.15 (d, $J=12$ Hz, 3H, COCH₃); 1.96–1.97 (m, $J=12$ Hz, 3H, CH₃); 125 (s, 3H, CH₃). Anal. Calcd. for C₃₃H₃₀N₄O₄S (578.69): C, 68.49; H, 5.23; N, 9.68%. Found: C, 65.88; H, 4.75; N, 9.41%.

2-[(7-Acetyl-4-cyano-1,6-dimethyl-6-hydroxy-8-(4-nitrophenyl)-5,6,7,8-tetrahydro-isoquinolin-3-yl)thio]-N-(naphthalen-1-yl)acetamide (8b)

It was synthesized by reaction of **2b** with *N*-(1-naphthyl)-2-chloroacetamide (IV). Yield: 93%; m.p.: 230–232 °C. The FT-IR spectrum of compound **8b**: 3604–3489 cm^{-1} for (O–H); 3356 cm^{-1} for (N–H); 3252(C–H, sp²); 2971, 2927 cm^{-1} for (C–H, sp³); 2218 cm^{-1} for (C≡N); 1705–1686 cm^{-1} for (C=Oamide, C=O acetyl). ¹H NMR spectrum of compound **8b** in (500 MHz, DMSO-d₆) show signals at δ : (500 MHz,) δ 10.23 (s, 1H, NH), 7.74–7.90 (m, 5H, Ar–H), 7.54–7.60 (m, 8H, Ar–H), 4.78–4.80 (d, $J=10.4$ Hz, 1H, OH), 4.33–4.47 (m, 2H, SCH₂), 3.46–3.47 (dd, $J=14.1, 7.0$ Hz, 1H, C⁸H), 3.32–3.35 (d, $J=17.1$ Hz, 1H, C⁵H), 2.95–2.98 (m, 2H, C⁷H and C⁵H), 2.17 (s, 3H, CH₃), 1.99–2.00 (d, $J=4$ Hz, 3H, CH₃), 1.30–1.31 (d, $J=4$ Hz, 3H, CH₃). ¹³C NMR spectrum of compound **8b** (DMSO-d₆) show environments of carbon as expected at δ : 208.5, 166.87, 165.62, 160.63, 157.87, 151.84, 150.08, 146.09, 133.69, 131.8, 128.16, 126.12, 126.00, 122.53, 122.52, 121.88, 121.88, 115.1, 104.19, 67.40, 65.7, 61.96, 56.06, 43.35, 31.17, 27.51, 24.63, 18.53. Anal. Calcd. for C₃₃H₃₀N₄O₄S (578.69): C, 68.49; H, 5.23; N, 9.68%. Found: C, 66.33; H, 4.92; N, 9.68%.

7-Acetyl-1-amino-N-(naphthalen-1-yl)-5,8-dimethyl-8-hydroxy-6-(3-Nitro phenyl)-6,7,8,9-tetrahydrothieno[2,3-c]isoquinoline-2-carboxamide (9a)

It was obtained by cyclization of compound **8a** Yield: 96%; m.p.: 290–293 °C. Color: yellow light powder. Recrystallized from ethanol. The FT-IR spectrum of compound **9a**: 3404 cm^{-1} for (O–H, NH₂, NH); 2922 cm^{-1} for (C–H, sp²); 2852 cm^{-1} for (C–H, sp³);

1707 cm^{-1} for (C=O, acetyl). ^1H NMR spectrum of compound **9a** in (90 MHz CDCl_3): δ 9.75 (1H, NH), 7.20–8.30 (11H, Ar–H), 6.70 (2H, NH_2), 3.6 (1H, OH), 2.70 (1H, C^6H), 2.40 (1H, C^9H) 2.10 (1H, C^9H), 1.90 (1H, C^7H), 1.35 (6H, CH_3 , COCH_3), 0.95 (3H, CH_3). Anal. Calcd for $\text{C}_{33}\text{H}_{30}\text{N}_4\text{O}_4\text{S}$ (578.69): C, 68.49; H, 5.23; N, 9.68%. Found: C, 69.1; H, 5.18; N, 9.52%.

7-Acetyl-1-amino-N-(naphthalen-1-yl)-5,8-dimethyl-8-hydroxy-6-(4-Nitro phenyl)-6,7,8,9-tetrahydrothieno[2,3-c]isoquinoline-2-carboxamide (9b).

It was obtained by cyclization of compound **8b** Yield: 89%; m.p.: 286–289 °C. Color: yellow light powder. Recrystallized from ethanol. The FT-IR spectrum of compound **9b**: 3481 cm^{-1} for (O–H, NH_2 , NH); 2956, 2924 cm^{-1} for (C–H, sp^2); 2853 cm^{-1} for (C–H, sp^3); 1706 cm^{-1} for (C=O, acetyl). ^1H NMR spectrum of compound **9b** in (90 MHz CDCl_3): δ 3.3 (s, 1H, NH), 7.00–8.40 (11H, Ar–H), 6.70 (br s, 2H, NH_2), 3.8 (s, 1H, OH), 2.20–22.30 (2H, C^9H , C^6H), 2.00 (1H, C^9H), 1.7 (1H, C^7H), 1.40 (s, 3H, CH_3 , at C-5), 1.20 (s, 3H, COCH_3), 1.00 (s, 3H, CH_3). Anal. Calcd for $\text{C}_{33}\text{H}_{30}\text{N}_4\text{O}_4\text{S}$ (578.69): C, 68.49; H, 5.23; N, 9.68%. Found: C, 69.33; H, 5.25; N, 9.59%.

Synthesis of 7-Acetyl-1-amino-N-(benzthiazol-2-yl)-5,8-dimethyl-8-hydroxy-6-(3-nitrophenyl)-6,7,8,9-tetrahydrothieno[2,3-c]isoquinoline-2-carboxamide (10)

It was obtained by reaction of **2a** (10 mmol) with *N*-(benzthiazol-2-yl)-2-chloroacetamide (**V**) (10 mmol), and sodium acetate trihydrate (1.50 g, 11 mmol) in ethanol (100 mL) was refluxed for one hour. The solid that formed after cooling was collected and then recrystallized from ethanol to give white crystals of compound **10** directly.

Yield: 97%; m.p.: 300–305 °C. FT-IR: 3431, 3319 cm^{-1} for (O–H, NH_2 , NH); 2973 cm^{-1} for (C–H, sp^2); 1707 cm^{-1} for (C=O, acetyl); ^1H NMR (400 MHz, DMSO-d_6) showed signals at δ : 7.22–8.08 (m, 11H, NH_2 , 11Ar–H), 4.86–4.88 (s, 2H, OH, C^9H), 3.65–3.68 (d, $J=12$ Hz, 1H, C^6H), 3.41–3.44 (d, $J=4$ Hz, 1H, C^7H), 2.90 (s, 1H, C^9H), 2.17 (s, 3H, COCH_3), 1.93 (s, 3H, CH_3), 1.34 (s, 3H, CH_3). ^{13}C NMR of compound **10** (dms) δ 209.47, 158.18, 157.84, 147.91, 147.12, 142.94, 135.08, 130.10, 127.91.67, 123.27, 123.1, 122.4, 121.50, 67.16, 65.93, 42.90, 41.97, 31.17, 27.98, 24.74, 18.53. Anal. Calcd. For $\text{C}_{29}\text{H}_{25}\text{N}_5\text{O}_5\text{S}_2$ (587.67): C, 59.27; H, 4.29; N, 11.92; O, 13.61; S, 10.91. Found C, 58.07; H, 4.35; N, 12.00.

Cytotoxicity against human cancer cell lines

Some of the synthesized compounds were tested as anti-cancer activity for the IC_{50} against two cell lines **HEPG2** and **MCF7** cells according to method [52, 81]. All cell

lines were obtained from national cancer institute, Cairo—Egypt.

Cell cycle analysis

The cell cycle arrests of compound **3** against **HEPG2** was carried out according to Abcam method (code ab139418), (www.abcam.co.jp) [52, 82, 83].

Annexin-V FITC apoptosis assay

The Annexin-V FITC apoptosis assay of compounds **3** against **HEPG2** was performed according to (BioVision Research Products (code k101-25). (www.biovision.com) [52, 84, 85].

Molecular docking Materials and Methods for RET Enzyme
Molecular docking studies were performed in (**I Mole Lab for Bioinformatics-Cairo**).

Ligand preparation

The retrieved Ligands structures were subjected to energy minimization using the Avogadro 1.2.0 software with the MMFF94 force field [86].

Protein target selection and preparation for RET enzyme

The selected target was the RET tyrosine kinase receptor was retrieved from data base (UniProt ID: Q9UMQ4). The protein structures were prepared using AutoDock Tools 1.5.7 [87].

Binding site identification for RET enzyme

The potential binding pockets on the selected protein targets were identified using the CB-Dock 2 webserver [88].

Molecular Docking for RET enzyme

Molecular docking studies were performed according to method [89].

Data analysis and visualization for RET enzyme

The results from molecular docking prediction were analyzed using appropriate computational tools and software. The visualization of protein–ligand interactions and the generation of figures were performed using Biovia 2020.

Ligand retrieval for HSP90 enzyme

Ligands Were retrieved from Pubchem using CID (Onalespib: 11955716) using SDF format, then all ligands were energy minimized using Avogadro 1.2.0 [90] software using MMFF94 force field due to Organic nature of compounds and saved using suitable Format.

Protein preparation for HSP90 enzyme

Proteins structure for, HSP90 enzyme was retrieved from data base uniprot ID (P08238), then protein prepared according to [87].

Molecular docking and visualization for HSP90 enzyme

Molecular docking simulation were performed using Autodock vina [91].

Conclusion

In this article, we synthesized and characterized a new tetrahydroisoquinoline compounds. Some of the synthesized compounds were examined for their anticancer activity towards HEPG2 and MCF7 cell lines. They showed high anticancer activities. Moreover, the cell cycle arrest and apoptosis induction of the one compounds was studied. Compound 3 caused cell cycle arrest of HEPG2 cell line at G2/M phase and caused high increase in the early and late apoptosis and necrosis. Furthermore, we applied the molecular docking study for compound 8a and it showed significant inhibition for RET enzyme while compound 3 exhibited high binding ability for HSP90 enzyme. This ensure the pervious article studies reported that tetrahydroisoquinoline compounds can be used as enzyme inhibitors.

Supplementary Information

The online version contains supplementary material available at <https://doi.org/10.1186/s13065-025-01399-0>.

Supplementary Material 1

Author contributions

Etify A. Bakhite: conceptualization, formal analysis, supervision, investigation. Reda Hassanien: investigation, methodology, writing–review & editing. Nasser Farhan: investigation, writing–original draft, writing–review & editing. Eman M. Sayed: investigation, methodology, writing–original draft, visualization, software, validation. Marwa Sharaky: conceptualization, formal analysis, supervision, investigation, methodology, writing–original draft, writing–review & editing.

Funding

Open access funding provided by The Science, Technology & Innovation Funding Authority (STDF) in cooperation with The Egyptian Knowledge Bank (EKB). This research received no funds.

Availability of data and materials

All data generated or analyzed during this study are in this published article and supplementary information and you can ask the corresponding author for any additional information's.

Declarations

Ethics approval and consent to participate

Not applicable.

Consent for publication

Not applicable.

Competing interests

The authors declare no competing interests.

Author details

¹Chemistry Department, Faculty of Science, Assiut University, Assiut 71516, Egypt. ²Chemistry Department, Faculty of Science, New Valley University, El-Kharja 72511, Egypt. ³Pharmacology Unit, Cancer Biology Department, National Cancer Institute, Cairo University, 12613, El-Gize, Egypt.

Received: 1 September 2024 Accepted: 27 January 2025

Published online: 21 February 2025

References

- Gaurav B, Ashima S, Jyoti T, Khurana JM. Design, synthesis and biological evaluation of spiroisoquinoline-pyrimidine derivatives as anticancer agents against MCF-7 cancer cell lines. *Results Chem.* 2022;4: Article No. 100386.
- Hanahan D, Weinberg RA. The hallmarks of cancer. *Cell.* 2000;100(1):57–70.
- WHO Global Cancer report 2015. <http://www.who.int/cancer/en/>.
- Dejene TD, Seke GYM, Kidist DH, Maureen TN, Betelhiem WM, Dagimawi CH, Sophia KK, Tsegahun M. New approaches and procedures for cancer treatment: current perspectives. *SAGE Open Med.* 2021;9: Article No. 20503121211034366.
- David A, Santosh KS, Shriti S, Varma S, Rajesh S. Challenges in liver cancer and possible treatment approaches. *Biochimica et Biophysica Acta (BBA) Rev Cancer.* 2020;1873(1): Article No. 188314.
- Yi-Hao Y, Kwong-Ming K, Wei L, Yueh-Wei L, Chih-Chi W, Tsung-Hui H, Ming-Chao T, Yuan-Hung K, Chih-Yun L. Causes of death among patients withhepatocellular carcinoma according to chronic liver disease etiology. *Cancers (Basel).* 2023;15(6): Article No. 1687.
- Estes C, Razavi H, Loomba R, Younossi Z, Sanyal AJ. Modeling the epidemic of nonalcoholic fatty liver disease demonstrates an exponential increase in burden of disease. *Hepatology.* 2018;67:123–33.
- Li J, Zou B, Yeo YH, Feng Y, Xie X, Lee DH, Fuji H, Wu Y, Kam LY, Ji F, et al. Prevalence, incidence, and outcome of non-alcoholic fatty liver disease in Asia: a systematic review and meta-analysis. *Lancet Gastroenterol Hepatol.* 2019;4:389–98.
- Isabelle S, Dian O, Valery L, Anke O, Vassiliki B, Antonia T, Jan W. Increased consumption of fruit and vegetables and future cancer incidence in selected European countries. *Eur J Cancer.* 2010;46(14):2563–80.
- Xiaojiayang L, Rong S, Rumping L. Natural products in licorice for the therapy of liver diseases: progress and future opportunities. *Pharmacol Res.* 2019;144:210–26.
- Yue Z, Ya L, Tong Z, Jie Z, Sha L, Hua-Bin L. Dietary natural products for prevention and treatment of liver cancer. *Nutrients.* 2016;8(3): Article No. 156.
- Seth BC, Karin E d V, Revving up dendritic cells while braking PD-L1 to jump-start the cancer-immunity cycle motor. *Immunity.* 2016;44(4):722–4.
- Yoav DL, Yehuda GA. Rationally designed nanovehicles to overcome cancer chemoresistance. *Adv Drug Deliv Rev.* 2013;65(13–14):1716–30.
- Gunasekaran V, et al. Targeting hepatocellular carcinoma with piperine by radical-mediated mitochondrial pathway of apoptosis: an in vitro and in vivo study. *Food Chem Toxicol.* 2017;105:106–18.
- Ming R, Lingyan Y, Xiaoshi H, Zhixing R, Shuping R, Kun X, Juan L. Polysaccharides from *Tricholoma matsutake* and *Lentinus edodes* enhance 5-fluorouracil-mediated H22 cell growth inhibition. *J Tradit Chin Med.* 2014;34(3):309–16.
- Xuemei D, Tian L, Zhao L, Huaixiu W, Honghua Z, Xiaoyan Y, Fang L, Dan L, Tao S, Quanyi Z, Zhen W. Design, synthesis and anti-hepatocellular carcinoma activity of 3-arylisquinoline alkaloids. *J Med Chem.* 2022;228: Article No. 113985.

17. Yuqing W, Lin L, Zhuo L, Honghua Z. Design, synthesis, and biological evaluation of 1-styrenyl isoquinoline derivatives for anti-hepatocellular carcinoma activity and effect on mitochondria. *Eur J Med Chem.* 2023;256: Article No. 115420.
18. Mahmoud IMD, Ahmed MM, Asmaa MY. Novel tetrahydro-[1,2,4] triazol[3,4-a]isoquinoline chalcones suppress breast carcinoma through cell cycle arrests and apoptosis. *Molecules.* 2023;28(8):3338.
19. Sung H, Ferlay J, Siegel RL, Laversanne M, Soerjomataram I, Jemal A, Bray F. Global cancer statistics 2020: GLOBOCAN estimates of incidence and mortality worldwide for 36 cancers in 185 countries. *CA Cancer J Clin.* 2021;71:209–49.
20. Chhikara BS, Parang K. Global cancer statistics 2022: the trends projection analysis. *Chem Biol Lett.* 2022;10(451):21.
21. Kozłowska J, Potaniec B, Żarowska B, Anioł M. Microbial transformations of 4'-methylchalcones as an efficient method of obtaining novel alcohol and dihydrochalcone derivatives with antimicrobial activity. *RSC Adv.* 2018;8:30379–86.
22. Feng-Yang W, Liang-Mei Y, Shan-Shan W, Hui L, Xu-Sheng W, Yuan L, Wen-Xiu N, Hong L, Ke-Bin H. Cycloplatinated (II) complex based on isoquinoline alkaloid elicits ferritinophagy-dependent ferroptosis in triple-negative breast cancer cells. *J Med Chem.* 2024;67(8):6738–48.
23. Florian HS, Maximilian MB, Johannes B. The HSP90 chaperone machinery. *Nat Rev Mol Cell Biol.* 2017;18:345–60.
24. Len N, Ivy SP. Heat shock protein 90. *Curr Opin Oncol.* 2003;15(6):419–24.
25. Huiyun W, Yingying Z, Yilin J, Xunan C, Tengda N, Aniruddha C, Pengxing H, Guiqin H. Heat shock protein 90: biological functions, diseases, and therapeutic targets. *MedComm.* 2024;5(2): e470.
26. Minh TL, Van-Hai H, Raghava S, Cong-T N, Gibeom N, Hyun-Ju P, Minsu P, Yoon-J K, Ji Young K, Jihyae A, Jae HS, Jeew L. Discovery of indazole inhibitors for heat shock protein 90 as anti-cancer agents. *Eur J Med Chem.* 2024;276: 116620.
27. Hamed WE, Rania MG, Shahenda ME, Fatma EG. Quinazoline based HSP90 inhibitors: synthesis modeling study and ADME calculations towards breast cancer targeting. *BMCL.* 2020;30: 127281.
28. Hamed WE, Rania MG, Shahenda ME, Fatma EG. Quinazoline based HSP90 inhibitors: synthesis, modeling study and ADME calculations towards breast cancer targeting. *Eur J Med Chem.* 2022;244: 114862.
29. Arun KM, Yulia AS. RET receptor tyrosine kinase: role in neurodegeneration, obesity, and cancer. *Int J Mol Sci.* 2020;21(19):7108.
30. Yunong Z, Shinpan C, Rui H, Yiling L, Xiaojuan S, Zheng-Chao T, Ren X, Yang Z, Zhang Z, Zhen W, Fengtao Z, Ke D. 1-Methyl-3-((4-(quinolin-4-yloxy)phenyl)amino)-1H-pyrazole-4-carboxamide derivatives as new rearranged during Transfection (RET) kinase inhibitors capable of suppressing resistant mutants in solvent-front regions. *Eur J Med Chem.* 2022;244: 114862.
31. Kisel VM, Kostyrko EO, Kovtunenka VA. Synthesis and biological properties of isoquinolines spirofused with carbocycles and heterocycles at position 4. *Chem Heterocycl Compd.* 2002;38:295–1318.
32. Potikha LM, Kovtunenka VA. Synthesis and properties of 3-aminodihydroisoquinolines. *Russ Chem Rev.* 2009;78:513–33.
33. Peukert S, Schwahn U, Gusstegen S, Schreuder H, Hofmeister A. Poly(ADP-Ribose) polymerase-1 (PARP-1) inhibitors based on a tetrahydro-1(2H)-isoquinolinone scaffold: synthesis, biological evaluation and X-ray crystal structure. *Synthesis.* 2005;5:1550–4.
34. Wu SC, Yoon D, Chin J, van Kirk K, Seethala R, Golla R, He B, Harrity T, Kunselman LK, Morgan NN, Ponticciello RP, Taylor JR, Zebo R, Harper TW, Li W, Wang M, Zhang L, Slecza BG, Nayeem A, Sheriff S, Camac DM, Mozin PE, Everlof JG, Li YX, Ferraro CA, Kiełtyka K, Shon W, Vath MB, Zvyaga TA, Gordon DA, Robl JA. Discovery of 3-hydroxy-4-cyanoisoquinolines as novel, potent, and selective inhibitors of human 11b-hydroxydehydrogenase 1 (11b-HSD1). *Bioorg Med Chem Lett.* 2011;21:6693–8.
35. Al-Omran F, Elassar AZA, El-Khair A. Synthesis of condensed heteroaromatics: novel synthesis of aminoquinolinone derivatives as anti-HIV agents. *Tetrahedron.* 2001;57:10163–70. [https://doi.org/10.1016/S0040-4020\(01\)01039-0](https://doi.org/10.1016/S0040-4020(01)01039-0).
36. Hsin LW, Chang LT, Rothman RB, Dersch CM, Fishback JA, Matsumoto RR. Synthesis and opioid activity of enantiomeric N-substituted 2,3,4,4a,5,6,7,7a-octahydro-1H-benzofuro[3,2-e]isoquinolines. *J Med Chem.* 2010;53:1392–6.
37. Chen L, Stefanac T, Turcotte N, Hu Z, Chen Y, Bedard J, May S, Jin H. Design and evaluation of dihydroisoquinolines as potent and orally bioavailable human cytomegalovirus inhibitors. *Med Chem Lett.* 2000;10:1477–80.
38. Paronikyan EG, Noravyan AS, Akopyan SF, Dzhagatspanyan IA, Nazaryan IM, Paronikyan RG. Synthesis and anticonvulsant activity of pyrano[4,3:4,5]pyrido[2,3-b]thieno[3,2-d]pyrimidine derivative's and pyrimido[5,4:2,3]thieno[2,3-c]isoquinoline derivatives. *Pharm Chem J.* 2007;41:466–9.
39. Paronikyan EG, Akopyan ShF, Noravyan AS, Gaiosh G, Sh DS, Paronikyan RV, Stepanyan GM. Synthesis and antibacterial activity of N- amino-derivatives of condensed pyridines. *Pharm Chem J.* 2013;47:257–60.
40. Paronikyan EG, Sh DS, Noravyan AS, Dzhagatspanyan IA, Paronikyan RG, Nazaryan IM, Akopyan AG. Synthesis and neurotropic activity of amino derivatives of cyclopenta[4,5]pyrido[3,2:4,5]thieno[3,2-d] pyrimidines and pyrimido[4,5:4,5]thieno[2,3-c]isoquinolines. *Pharm Chem J.* 2016;50:301–5.
41. Kamal AM, Radwan SM, Zaki RM. Synthesis and biological activity of pyrazolothienotetrahydroisoquinoline and [1,2,4]triazolo[3,4-a]thienotetrahydro-isoquinoline derivatives. *Eur J Med Chem.* 2011;46:567–78.
42. Gangapuram M, Eyunni S, Redda KK. Synthesis and pharmacological evaluation of tetrahydroisoquinolines as anti breast cancer agents. *J Cancer Sci Ther.* 2014;6(5):161–9.
43. Gao Y, Tu N, Liu X, Lu K, Chen S, Guo J. Progress in the total synthesis of antitumor tetrahydroisoquinoline alkaloids. *Chem Biodiversity.* 2003;20(5): Article No. e202300172.
44. Faheem KK, Chandra S, Chander S, Kunjiappan S, Murugesan S. Medicinal chemistry perspective of 1,2,3,4-tetrahydroisoquinoline analogs biological activities and SAR studies. *RSC Adv.* 2021;11(20):12254–87.
45. Ju KS, Parales RE. Nitroaromatic compounds, from synthesis to biodegradation. *Microbiol Mol Biol Rev.* 2010;74:250–72.
46. Noboru O. The nitro group in organic synthesis. Weinheim: Wiley VCH; 2001. p. 1–363.
47. Strauss M. The nitroaromatic group in drug design. *Ind Eng Chem Prod Res Dev.* 1979;18:158–66.
48. Nepali K, Lee HY, Liou JP. Nitro-group-containing drugs. *J Med Chem.* 2019;62:2851–93.
49. Eman MS, Hassanien R, Mohamed SK, Mague JT, Akkurt M, Farhan N, Bakhite EA, Al-Waleedy SAH. Crystal structure and Hirshfeld surface analysis of 2-[[7-acetyl-4-cyano-6-hydroxy-8-(4-methoxyphenyl)-1,6-dimethyl-5,6,7,8-tetrahydroisoquinolin-3-yl]sulfonyl]-N-phenylacetamide. *Acta Cryst.* 2021;E77:663–7.
50. Eman MS, Reda H, Nasser F, Hanan FA, Khaled M, Shaaban KM, Joel TM, Etify AB. Nitrophenyl-group-containing heterocycles. Part I. Synthesis, characterization, anticancer activity and antioxidant properties of some new 5,6,7,8-tetrahydro-isoquinolines bearing 3(4)-nitrophenyl group. *ASC Omega.* 2022;7(1):8767–76.
51. Eman MS, Etify AB, Reda H, Nasser F, Hanan FA, Salma GM, Nivin AH. Novel tetrahydroisoquinolines as DHFR and CDK2 inhibitors: synthesis, characterization, anticancer activity and antioxidant properties. *BMC Chem.* 2024;18(1): Article No. 34.
52. Abdelreheem AS, Etify AB, Reda H, Nasser F, Eman MS, Marwa S. Some new 5,6,7,8-tetrahydro-isoquinolines bearing 2-nitrophenyl group targeting RET enzyme: synthesis, anticancer activity, apoptotic induction and cell cycle arrest. *chem. Biodiversity.* 2024. <https://doi.org/10.1002/cbdv.202402758>.
53. Rashidi M, Seghatoleslam A, Namavari M, et al. Selective cytotoxicity and apoptosis-induction of cyrtopodium scabrum extract against digestive cancer cell lines. *IJCM.* 2017;10: e8633.
54. Tronina T, Bartmańska A, Popłoński J, Wietrzyk A, Huszcza E. Prenylated flavonoids with selective toxicity against human cancers. *Int J Mol Sci.* 2023;24:7408.
55. Watanuki S, Matsuura K, Tomura Y, et al. Synthesis and pharmacological evaluation of 1-isopropyl-1,2,3,4-tetrahydroisoquinoline derivatives as novel antihypertensive agents. *Chem Pharm Bull.* 2011;59:1029–37.
56. Pingaew R, Prachayasittiku S, Ruchirawat S. Synthesis, cytotoxic and anti-malarial activities of benzoyl thiosemicarbazone analogs of isoquinoline and related compounds. *Molecules.* 2010;15:988–96.
57. Hassaneen HM, Wardkhan WW, Mohammed YS. A novel route to isoquinoline[2, 1-g][1,6]naphthyridine, pyrazolo[5,1-a] isoquinoline and pyridazino[4',5':3,4]pyrazolo[5, 1-a]isoquinoline derivatives with evaluation of antitumor activities. *Naturforsch.* 2013;68:895–904.

58. Kakhki S, Shahosseini S, Zarghi A. Design, synthesis and cytotoxicity evaluation of new 2-aryl-5,6-dihydropyrrolo[2,1-a] isoquinoline derivatives as topoisomerase inhibitors. *Iran J Pharm Res.* 2014;13:71–7.
59. Cushman M, Jayaraman B, Vroman JA, et al. Synthesis of new indeno[1,2-c]isoquinolines: cytotoxic non-camptothecin topoisomerase I inhibitors. *J Med Chem.* 2000;43:3688–98.
60. Rashad AS, Ibrahim A, Mohamed M. Cytotoxicity evaluation of a new set of 2-aminobenzo[de]isoquinoline-1,3-diones. *Int J Mol Sci.* 2014;15:22483–91.
61. Mohassab AM, Hassan HA, Abdelhamid D, et al. Design and synthesis of novel quinoline/chalcone/1,2,4-triazole hybrids as potent antiproliferative agent targeting EGFR and BRAFV600E kinases. *Bioorg Chem.* 2021;106:104510.
62. Abdelsalam EA, Zaghary WA, Amin KM, et al. Synthesis and invitro anticancer evaluation of some fused indazoles, quinazolines and quinolines as potential EGFR inhibitors'. *Bioorg Chem.* 2019;89:102985.
63. Tang Q, Duan Y, Xiong H, et al. Synthesis and antiproliferative activity of 6,7-disubstituted-4-phenoxyquinoline derivatives bearing the 1,8-naphthyridin-2-one moiety. *Eur J Med Chem.* 2018;158:201–13.
64. Mikiko I, Jingyang L, Kenji M. Cell chirality: its origin and roles in left-right asymmetric development. *Philos Trans R Soc Lond B Biol Sci.* 2016;19:20150403.
65. Ashish KP, Bir B. Chirality in nature and biomolecules: an overview. *Int J Life Sci.* 2020;9:72–84.
66. Liting G, Yanqiu G, Rui W, et al. Interface chirality: from biological effects to biomedical applications. *Molecules.* 2023;28:5629.
67. Akkurt M, Marae IS, Mague JT, Mohamed SK, Bakhite EA, Al-Waleedy SAH. Crystal structure and hirshfeld surface analysis of 2-[[7-acetyl-8-(4-chlorophenyl)-4-cyano-6-hydroxy 1,6-dimethyl-5,6,7,8-tetrahydroisoquinolin-3-yl]sulfanyl]-n-(4-chlorophenyl)acetamide. *Acta Crystallogr A.* 2021;E77:527–31.
68. Mague JT, Al-Taifi EA, Mohamed SK, Akkurt M, Bakhite EA. "Methyl 2-[[[(6S*,7R*,8S*)-7-acetyl-8-(4-chlorophenyl)-4-cyano-6-hydroxy-1,6-dimethyl-5,6,7,8-tetrahydroisoquinolin-3-yl]sulfanyl]acetate. *IUCr Data.* 2017;2: x170868.
69. Mague JT, Mohamed SK, Akkurt M, Bakhite EA, Albayatif MR. 6-Acetyl-8-(4-chlorophenyl)-3-ethylsulfanyl-6-hydroxy-1,6-dimethyl-5,6,7,8-tetrahydro-isoquinoline-4-carbonitrile. *IUCr Data.* 2017;2: x170390.
70. Ashraf AA, Esmat ME, Momtaz EMB, Mai AEM, Stefan B, Mahmoud AAI, Martin N, Boyan KG, Kevin ND, Tamer SK. Design, synthesis and biological evaluation of fused naphthofuro[3,2-c] quinoline-6,7,12-triones and pyrano[3,2-c] quinoline-6,7,8,13-tetraones derivatives as ERK inhibitors with efficacy in BRAF-mutant melanoma. *Bioorg Chem.* 2019;82:290–305.
71. Vyas VK, Qureshi G, Oza D, et al. Synthesis of 2-,4-,6-, and/or 7-substituted quinoline derivatives as human dihydroorotate dehydrogenase (hDHODH) inhibitors and anticancer agents: 3D QSAR-assisted design. *BMCL.* 2019;29:917–22.
72. Perin N, Nhili R, Cindrić M, et al. Amino substituted benzimidazo[1,2-a] quinolines: antiproliferative potency, 3D QSAR study and DNA binding properties. *Eur J Med Chem.* 2016;122:530–45.
73. Ribeiro AG, Almeida SMV, Oliveira JF, et al. Novel 4-quinoline-thiosemicarbazone derivatives: synthesis, antiproliferative activity, in vitro and in silico biomacromolecule interaction studies and topoisomerase inhibition. *Eur J Med Chem.* 2019;182: 111592.
74. Vennila KN, Sunny D, Madhuri S, Ciattini S, Chelazzi L, Elango KP. Design, synthesis, crystal structures and anticancer activity of 4-substituted quinolines to target PDK1. *Bioorg Chem.* 2018;81:184–90.
75. Elbadawi MM, Eldehna WM, Wang W, Agama KK, Pommier Y, Abe M. Discovery of 4-alkoxy-2-aryl-6,7-dimethoxyquinolines as a new class of topoisomerase I inhibitors endowed with potent in vitro anticancer activity. *Eur J Med Chem.* 2021;215: 113261.
76. Karnik KS, Sarkate AP, Tiwari SV, Azad R, Burra PVLS, Wakte PS. Computational and synthetic approach with biological evaluation of substituted quinoline derivatives as small molecule L858R/T790M/C797S triple mutant EGFR inhibitors targeting resistance in non-small cell lung cancer (NSCLC). *Bioorg Chem.* 2021;107: 104612.
77. Aly RM, Serya RAT, El-Motwally AM, Esmat A, Abbas S, Abou El Ella DA. Novel quinoline-3-carboxamides (part 2): design, optimization and synthesis of quinoline based scaffold as egfr inhibitors with potent anticancer activity. *Bioorg Chem.* 2017;75:68–392.
78. Kairuki M, Qiu Q, Pan M, et al. Designed P-glycoprotein inhibitors with triazol-tetrahydroisoquinoline-core increase doxorubicin induced mortality in multidrug resistant K562/A02 cells. *Bioorg Med Chem.* 2019;27:3347–57.
79. Sabrin RMI, Gamal A. Mohamed naphthylisoquinoline alkaloids potential drug leads. *Fitoterapia.* 2015;106:194–225.
80. Anil K, Anurad PD, Sudhak M, Madhuri S. Ancistrocline: a naphthyl isoquinoline alkaloid from the leaves of *Ancistrocladus heyneanus*: exhibits anticancer property against Plc/Prf/5, Hepatoma Cells. *IJFMR.* 2024;7. <https://doi.org/10.36948/ijfmr.2024.v06i03.22144>.
81. Tarfah A, Ahmed AA, Ayman AE, Maha AA, Marwa A, Taghreed AM, Medhat A, Ahmed N, Wagdy ME, Marwa S. Biological evaluation, docking studies, and in silico ADME prediction of some pyrimidine and pyridine derivatives as potential EGFRWT and EGFR T790M inhibitors. *J Enzyme Inhib Med Chem.* 2023;38(1):176–91.
82. Lili X, Guozheng H, Zhihui Z, Shasha T, Yingying W, Huanwu H, Xiaowei L, Ying L, Feize L, Huajun Z. LFZ-4-46, a tetrahydroisoquinoline derivative, induces apoptosis and cell cycle arrest via induction of DNA damage and activation of MAPKs pathway in cancer cells. *Anticancer Drugs.* 2021;32(8):842–54.
83. Megda FM, Hamdi MH, Ismail AA. Cytotoxicity, molecular modeling, cell-cycle arrest and apoptotic induction induced by novel tetrahydro [1,2,4] triazolo[3,4-a] isoquinoline chalcones. *Eur J Med Chem.* 2018;143:532–41.
84. Mohammed FZ, Rizk YW, El Deen IM, Mourad AAE, El Behery M. Design, synthesis, cytotoxic screening and molecular docking studies of novel hybrid thiosemicarbazone derivatives as anticancer agents. *Chem Biodiv.* 2021;18: Article No. e2100580.
85. Mohammed F, Rizk YW, Mohey El-Deen I, Gad EM, El Behery M, Mahdy ARE. Discovery of 2-amino-4h-1,3, 4-thiadiazine-5(6H)-one derivatives and their in vitro antitumor investigation. *Med Chem Drug Dis.* 2022;7: Article No. 246962242.
86. Marcus DH, Donald EC, David CL, Tim V, Eva Z, Geoffrey RH. Avogadro: an advanced semantic chemical editor, visualization, and analysis platform. *J Chem Inf.* 2012. <https://doi.org/10.1186/1758-2946-4-17>.
87. Morris GM, Huey R, Lindstrom W, et al. AutoDock4 and AutoDockTools4: automated docking with selective receptor flexibility. *J Comput Chem.* 2009;16:2785–2791.
88. Liu Y, Yang X, Gan J, Chen S, Xiao ZX, Cao Y. CB-Dock 2: improved protein-ligand blind docking by integrating cavity detection, docking and homologous template fitting. *Nucleic acids res.* 2022;50:W159–64.
89. Eberhardt J, Santos-Martins D, Tillack AF, Forli S. AutoDock Vina 1.2.0: new docking methods, expanded force field, and python bindings. *J Chem Inf Model.* 2021;61:3891–8.
90. Hanwell MD, Curtis DE, Lonie DC, Vandermeersch T, Zurek E, Hutchison GR. Avogadro: an advanced semantic chemical editor, visualization, and analysis platform. *J Cheminf.* 2012;4(1):1–17.
91. Trott O, Olson AJ. AutoDock Vina: improving the speed and accuracy of docking with a new scoring function, efficient optimization, and multi-threading. *J Comput Chem.* 2010;31(2):455–61.

Publisher's Note

Springer Nature remains neutral with regard to jurisdictional claims in published maps and institutional affiliations.